

Low temperature heat capacity of amorphous systems: physics at nano-scales

Pragya Shukla

Department of Physics, Indian Institute of Technology, Kharagpur-721302, India

(Dated: March 23, 2022)

Abstract

Contrary to previous studies of boson peak, we analyze the density of states and specific heat contribution of dispersion forces in an amorphous solid of nano-scales ($\sim 3nm$). Our analysis indicates a universal semi-circle form of the average density of states in the bulk of the spectrum along with a super-exponentially increasing behavior in its edge. The latter in turn leads to a specific heat, behaving linearly below $T < 1^o \text{ K}$ even at nano-scales, and, surprisingly agreeing with the experiments although the latter are carried out at macroscopic scales. The omnipresence of dispersion forces at microscopic scales indicates the application of our results to other disordered materials too.

I. INTRODUCTION

At low temperatures, structurally and orientationally disordered solids such as dielectric and metallic glasses, amorphous polymers and even crystals are experimentally observed to exhibit many universalities [1–3]. Initially the origin of this behavior was attributed to the tunnelling two level systems (TTLS) intrinsic to disordered state [4, 5]. The existence of TTLS entities however in a wide range of materials is not well-established (besides many other issues e.g. see [6–17]). Previous attempts in search of alternative theoretical explanations led to introduction of many new models e.g. soft potential model [18–21], heterogeneous elasticity theory [22, 23], Euclidean random matrices [24], effective medium theories and jamming approach (e.g. [25, 26] and references therein), correlations at microscopic scales [27–30] and several others [31–37] but almost none of these studies analyzed the existence of universalities at nanoscales [7]. With increasing industrial significance of nano materials, it becomes imperative to seek the information whether these glass peculiarities emerge only at macro-sizes (with experimental sample size typically $\sim 1\text{ cm}^3$) or exist at nano-scales too? and if not then when and how much they deviate? The primary focus of the present work is to bridge this information gap by an analysis of the density of states and low temperature specific heat at these scales.

The appearance of similar universal features in a wide range of disordered systems strongly suggest the behavior to originate in fundamental type of interactions. This intuitively motivates us to consider the inter-molecular interactions, more specifically the Vanderwaal (VW) forces among the molecules of the amorphous solid as the root cause for the behavior. The intuition comes from the omnipresence of these forces in all condensed phases thus making them promising candidates to decipher the experimentally observed universality.

Amorphous solids possess a rich and varied array of short to medium range topological order which originates from their chemical bonding and related interactions. The bonding interactions at short range (upto 1st and 2nd nearest neighbor molecular distances), are dictated by the valance force fields (covalent or ionic, also acting as mechanical constraints) but the medium range order (typically of the order of $10 - 30\text{ \AA}$), is governed by the VW interactions [38, 39]. Intuitively these varying structures at different length scales

are expected to result in materials with very different physical properties. Any theory of experimentally observed universality therefore must take into account the microscopic structure of the solid and explain the emergence of system-independence of the physical properties at large scales; this is because the related experiments are usually carried out on macroscopic sizes. The point to ponder is whether the observed universalities are emergent phenomenon due to interactions at larger scale or even the molecular interactions within the short length scales (of medium range order) can give rise to them on their own. The query arises because the nano-materials exhibit physical and chemical properties that are significantly different from the corresponding properties of bulk materials [40–44]. It is therefore relevant to seek, identify and analyze the behavior of the sub-units (nano-scale structures, later referred as basic blocks) of the macroscopic glass solid.

Our primary focus in the present work is to understand the low temperature behavior of the specific heat for one such subunit i.e a nano-size glass sample. Based on the standard partition function approach, this requires a prior knowledge of the density of states and therefore its Hamiltonian \mathcal{H} . The latter, although acting in an infinite dimensional Hilbert space, can be represented by a large but finite-size matrix in a physically motivated basis, with the size dictated by energy-range of interactions. Due to complexity of the many-body interactions within the block, however, the matrix elements can not be exactly determined and can at best be described by their distribution over an ensemble of the replicas of H -matrix. Intuitively, the form of the distribution or the distribution parameters are expected to be system specific. The experimentally observed universality at low temperatures however suggests that the theoretical formulation should not depend on any system-specific details. We therefore will not assume any specific form of the distribution of the elements of H -matrix except that the latter must satisfy basic symmetry and conservation laws of the Hamiltonian.

The paper is organized as follows. Section II describes the Hamiltonian of a basic block as a collection of molecules and calculates the variance of its matrix elements in a physically motivated basis. The latter information is used in section III to derive the ensemble averaged density of states of the Hamiltonian which turns out to be a semi-circle in the bulk of the spectrum but growing super-exponentially in its edge. As the density is derived without using any system-specific information about the intra-molecular forces, it is applicable for a wide range of glasses including the network as well as the metallic ones. Section IV derives

the specific heat of the basic block for the temperature ranges below and above Debye temperature and confirms its linear/superlinear temperature dependence even at nanoscale sizes. We conclude in section V with a summary of our main ideas, results and a brief comparison with some existing theories.

II. BASIC BLOCK HAMILTONIAN

An appropriate description of the Hamiltonian of the basic block requires a prior knowledge of the microscopic structure in amorphous materials. With both crystalline and non-crystalline materials sharing similar structure at SRO and their difference emerging at MRO, intuitively the latter seems to be the most potential candidate to explain their differences. This motivates us to consider the Hamiltonian which governs the dynamics of amorphous molecules at MRO only and can be described as follows.

A. The operator and Intermolecular interactions

The atoms at short range order, in both crystalline and non-crystalline material, are held together by strong covalent/ ionic bonds and form the "basic structural unit" that plays an important role in their physical properties. Consider a nano-size block of an arbitrary isotropic amorphous material, composed of g_0 molecules labeled as " k " with positions \mathbf{r}_k and masses m ; each molecule here refers to the basic structural unit in the amorphous system (e.g SiO_4 tetrahedra in case of SiO_2 glass, BO_3 in case of Borate glass) and is therefore polyatomic. The Hamiltonian of the block can be written as

$$\mathcal{H} = \mathcal{H}_0 + \mathcal{U}(\mathbf{r}_1, \mathbf{r}_2, \dots, \mathbf{r}_{g_0}) \quad (1)$$

where \mathcal{H}_0 is the total Hamiltonian of g_0 uncoupled (or free) molecules

$$\mathcal{H}_0 = \sum_{n=1}^{g_0} h_n(\mathbf{r}_n) \quad (2)$$

with $h_n(\mathbf{r}_n)$ as the Hamiltonian of the n^{th} molecule at position \mathbf{r}_n , consisting of its kinetic energy and the intra-molecular interactions, and, \mathcal{U} as the sum over inter-molecular many-body interactions of g_0 molecules.

Phenomenologically intermolecular (atomic) interactions can be described as occurring between permanent and instantaneous dipoles [45]. For non-polar molecules, the dominant

contribution arises from quantum induced instantaneous dipole-induced dipole interactions (referred as dispersion forces in short) and caused by correlated movements of electrons in interacting molecules. In an attempt to avoid each other at short intermolecular distances, a redistribution of electrons that belong to different molecules leads to formation of instantaneous dipoles that attract each other. The dispersion forces have variable strengths depending on size, shape and polarisability of the molecules. In case of molecules with permanent dipole moments, one also needs to consider other types of VW forces i.e Debye forces (permanent dipole-induced dipole interaction, also referred as induction forces) and Keesom forces (interactions among permanent dipoles that are ensemble averaged over different rotational orientations of the dipoles). The dispersion force however contribute the most to overall inter-molecule bonding even in presence of other electrostatic interactions e.g. hydrogen bonding or Keesom interaction [45]. For separations $R \geq 10 - 15 \text{ \AA}$ between the molecules, electron exchange effects are negligible and the contributions to the intermolecular energy, except for the unimportant magnetic terms, derive primarily from the Coulombic interactions between their particles [45, 52, 56]. As discussed in section 4.1 of [45], \mathcal{U} can be written in terms of the charge-density operator $\rho^{(m)}(\mathbf{r})$ of the molecules, $m = 1 \rightarrow g_0$:

$$\mathcal{U} = \sum_{\substack{m,n \\ m \neq n}} \int \frac{\rho^{(m)}(\mathbf{r}) \rho^{(n)}(\mathbf{r}')}{|\mathbf{r} - \mathbf{r}'|} d\mathbf{r} d\mathbf{r}' \quad (3)$$

The above formulation, although exact, is not the best framework for analysis. Alternative formulations e.g. perturbation or abinitio approaches have turned out to be quite successful in predicting the effect of these forces on physical properties [45]. The inter-molecular interactions being relatively weaker as compared to intra-molecular ones, \mathcal{U} can be considered as a perturbation on \mathcal{H}_0 and expanded as a series consisting of n -body contributions [45, 46]

$$\mathcal{U} = \mathcal{U}^{es} + \sum_{j=2}^{\infty} \mathcal{U}_j \quad (4)$$

where \mathcal{U}_{es} corresponds to 1st order perturbation correction consisting only of electrostatic contribution. The term \mathcal{U}_j refers to the j^{th} order perturbation correction arising only from the polarization interactions (i.e induction and dispersion) among j or more molecules. For later use, it is however better to rewrite the above series in terms of the n -body contributions,

referred as $\mathcal{U}^{(q^1, q^2, \dots, q^n)}$ (arising from polarization interactions among n molecules, labeled as " q^1 ", " q^2 " ..., " q^n "):

$$\mathcal{U}(\mathbf{r}_1, \dots, \mathbf{r}_{g_0}) = \mathcal{U}^{es}(\mathbf{r}_1, \dots, \mathbf{r}_{g_0}) + \sum_{n=2}^{g_0} \sum_{q^1, q^2, \dots, q^n} \mathcal{U}^{(q^1, q^2, \dots, q^n)}(\mathbf{r}_{q^1}, \dots, \mathbf{r}_{q^n}) \quad (5)$$

Here the symbol $\sum_{q^1, q^2, \dots, q^n}$ corresponds to a summation over all possible n -body polarization interactions (i.e including both dispersion as well as induction) among all g_0 molecules.

B. Matrix Representation

For matrix representation of \mathcal{H} , we consider the eigen-basis of the non-interacting molecules, consisting of the direct-product of g_0 normalised single-molecule states in which the molecules are assigned to definite single-molecule states; (hereafter the basis will be referred as NIM). In general a single molecule can exist in infinitely many states of electronic, vibrational and rotational type; this would imply an infinite dimensional basis-space. To study the thermal effects at very low temperatures ($T < 30K$), it is however sufficient to consider only roto-vibrational levels in the electronic ground state of each isolated molecule [47]. Assuming only \mathcal{N} such states of each molecule participate in the interaction, this gives the size of NIM basis space as

$$N = \mathcal{N}^{g_0}. \quad (6)$$

Let $|\mathcal{K}_n\rangle$ and $E_{\mathcal{K}_n} = \langle \mathcal{K}_n | h_n | \mathcal{K}_n \rangle$, with $\mathcal{K}_n = 1, 2, \dots, \mathcal{N}$ be the eigenvectors and eigenvalues of a molecule, say " n " with its Hamiltonian as h_n . A typical basis-state in the $N \times N$ dimensional NIM basis can then be given as

$$|\mathcal{K}\rangle = \prod_{n=1}^{g_0} |\mathcal{K}_n\rangle \quad (7)$$

with $|\mathcal{K}_n\rangle$ referring to the specific eigenvector of the n^{th} molecule which occurs in the product state $|\mathcal{K}\rangle$. (Note as the exchange interactions are neglected, the basis need not be anti-symmetrized). From eq.(2), \mathcal{H}_0 is a diagonal matrix in the NIM basis

$$\mathcal{H}_{0; \mathcal{K}L} \equiv \langle \mathcal{K} | \mathcal{H}_0 | \mathcal{L} \rangle = \sum_{n=1}^{g_0} E_{\mathcal{K}_n} \delta_{\mathcal{K}L} \quad (8)$$

Eq.(5) leads to the element $\mathcal{U}_{\mathcal{KL}} \equiv \langle \mathcal{K} | \mathcal{U} | \mathcal{L} \rangle$ corresponding to interaction energy for transition from state \mathcal{K} to \mathcal{L} . Due to $\mathcal{U}^{(q1,q2,\dots,qn)}$ being a n -body interaction among the molecules, the NIM basis has selection rules associated with a n -body interaction; only n molecules labeled as " $q1, q2, \dots, qn$ " can be transferred by H to different single-molecule states; Its matrix element between basis states $|\mathcal{K}\rangle$ to $|\mathcal{L}\rangle$ can then be given as

$$\mathcal{U}_{\mathcal{KL}}^{(q1,q2,\dots,qn)} = \langle \mathcal{K} | \mathcal{U}^{(q1,q2,\dots,qn)} | \mathcal{L} \rangle = \mathcal{F}_{\mathcal{KL}}^{(q1,q2,\dots,qn)} D_{\mathcal{KL}}^{(q1,q2,\dots,qn)} \quad (9)$$

where $\mathcal{F}_{\mathcal{KL}}^{(q1,q2,\dots,qn)}$ is a function dependent on polarisability of the molecules " $q1$ ", " $q2$ ", .. " qn " as well as their separation and

$$D_{\mathcal{KL}}^{(q1,q2,\dots,qn)} = \prod_{\substack{q=1 \\ q \neq q1,q2,\dots,qn}}^{g_0} \delta_{\mathcal{K}_q, \mathcal{L}_q} \quad (10)$$

As clear from the above, the matrix element in eq.(9) is non-zero only if the basis-pair $|\mathcal{K}\rangle, |\mathcal{L}\rangle$ have same contributions from the rest $g_0 - n$ molecules (excluding those labeled by " $q1, q2, \dots, qn$ "); we henceforth refer a pair $|\mathcal{K}\rangle, |\mathcal{L}\rangle$ as p -plet if they differ in eigenfunction contributions from p -molecules i.e $\mathcal{K}_m \neq \mathcal{L}_m$ with m taking p -values from the set $\{1, 2, \dots, g_0\}$. Clearly the total number of states $|\mathcal{L}\rangle$ forming a p -plet with a fixed $|\mathcal{K}\rangle$ is $(1/2)g_0!(g_0-1)!\mathcal{N}^p$.

As the induction and dispersion interaction result in transition of molecules from one state to another, they contribute only to off-diagonal matrix elements (see chapter 4 of [45]). From eq.(5), the matrix element $\mathcal{U}_{\mathcal{KL}}$ can be written as

$$\mathcal{U}_{\mathcal{KL}} = \delta_{\mathcal{KL}} \mathcal{U}_{\mathcal{KL}}^{es} + (1 - \delta_{\mathcal{KL}}) \left(\sum_{\substack{m,n \\ m>n}} \mathcal{U}_{\mathcal{KL}}^{(mn)} + \sum_{\substack{m,n,r \\ m>n>r}} \mathcal{U}_{\mathcal{KL}}^{(mnr)} + \sum_{\substack{m,n,r,s \\ m>n>r>s}} \mathcal{U}_{\mathcal{KL}}^{(mnrs)} + \dots \right) \quad (11)$$

For \mathcal{K}, \mathcal{L} pair forming a p -plet (for $p > 0$), $\mathcal{U}_{\mathcal{KL}}$ has contribution from all $p + x$ body terms with $x \geq 0$ (i.e $p \leq p + x \leq g_0$) (see *appendix F*). Although an exact calculation of these matrix elements is possible only for simple molecules, they can be approximated by some well-established methods e.g. using model potentials or by a multi-pole expansion of the n -body operator; the coefficients of expansions are then determined by abinitio approaches [45].

C. Statistics of the Matrix Elements

From eq.(8), the diagonal matrix elements of \mathcal{H} in the NIM basis are a sum over single molecule energy levels. As the molecules considered here are typically polyatomic, the

couplings between various degrees of freedom (e.g electronic, vibrational, nuclear) of a single molecule can not be ignored even for low lying energy states [49]. This in turn renders the description of each energy level by a set of quantum numbers often very difficult and meaningless, leaving a statistical analysis of the spectrum as the only option. The basic prerequisite of such an analysis, i.e the availability of a sufficiently large data set of energy levels of a single molecule is again experimentally not feasible [49]. This has motivated in past consideration of the ensemble averaging [49] (also see section 4.2.2 of [61]) which can be justified on following grounds (in the regime where levels can not be associated with exact quantum numbers): although the particle-interactions within a single molecule are not random by themselves, the missing information due to complexity of the many body interactions leads to randomization of the matrix elements of the Hamiltonian in a physically motivated basis. As a consequence, the energy levels and the eigenstates intensities can at best be described by the probability distribution. (Note similar ideas used by Wigner in nuclear spectroscopy led to random matrix modelling of complex nuclei, atoms and molecules [61]). The application of modern laser spectroscopy to resolve the enormously rich and complex spectra of such molecules has indicated that the statistics for the *irregular* part of the spectrum can be well-described by the random matrix ensembles [49] (also see section 4.2.2 of [61] for a review of the random matrix applications of molecules). Even for the regular part (described by exact quantum numbers), the underlying symmetries result in large number of degeneracies and lead to Poisson distribution of the energy levels [49, 61]. The appearance of randomness due to underlying complexity is also supported by the detailed numerical investigations, indicating that a typical eigenstate of the molecule in a physically motivated basis (which preserves the symmetry constraints of h_n) is randomly distributed, (localized or extended in the basis, subjected to symmetry constraints). As a NIM basis-state (eq.(7)) is a product of single molecule states, it is also expected to be a random function.

The $N \times N$ matrix \mathcal{U} in the NIM basis has total $N(N + 1)/2$ elements given by eq.(11), with $N = \mathcal{N}^{g_0}$ however many of them zero due to forbidden dipole transitions. With $N {}^{g_0}C_p \eta^p$ as the total number of basis-pairs forming p -plets ($\eta = \mathcal{N} - 1$ as the number of allowed dipole transitions in a single molecule), the number of non-zero off-diagonals can be given as $N \sum_{p=1}^{g_0} {}^{g_0}C_p \eta^p$. This implies \mathcal{U} is, in principle, a sparse matrix. But as the total number of non-zero off-diagonals is much larger than the diagonals, it effectively behaves as a dense matrix. (Note, although the matrix elements corresponding to p -plets, with p large,

are relatively weaker but their total number compensates for the weakness).

Further, due to instantaneous nature of the interaction, \mathcal{U}_{kl} is subjected to system dependent fluctuations; this in turn leads to randomization of the matrix elements of \mathcal{H}_{kl} . As a consequence, the behavior of the "Hamiltonian" \mathcal{H} is best described by an ensemble of \mathcal{H} -matrices, consisting of the independent ensembles of \mathcal{H}_0 and \mathcal{U} -matrices. As eq.(8 indicates, H_0 is an ensemble of diagonal matrices, with each diagonal as a superposition of g_0 single molecule energies. With help of eqs.(8,9), the ensemble average of the matrix element $\mathcal{H}_{KL} = \mathcal{H}_{0KL} + \mathcal{U}_{KL}$ can be written as

$$\langle \mathcal{H}_{KL} \rangle = \sum_{n=1}^{g_0} \langle \mathcal{H}_{0;K_n}^{(n)} \rangle \delta_{KL} + \langle \mathcal{U}_{KL} \rangle = \sum_{n=1}^{g_0} \langle E_{K_n} \rangle \delta_{KL} + \langle \mathcal{U}_{KL} \rangle \quad (12)$$

where $\langle \mathcal{U}_{KL} \rangle$ is given by an ensemble average of eq.(11).

A typical many body contribution can be both attractive as well as repulsive type and depends on the mutual orientation of the molecules and, as clear from the above, $\langle \mathcal{U}_{KL} \rangle$ is a sum over many such contributions. Under conditions in which all mutual orientations of the molecules are equally probable, the average of \mathcal{U}_{KL} over an ensemble of molecules can then safely be assumed to be zero: $\langle \mathcal{U}_{KL} \rangle \approx 0$. Eq.(12) along with eq.(11) then gives

$$\langle \mathcal{H}_{KL} \rangle \approx a_K \delta_{KL}, \quad a_K = \sum_{n=1}^{g_0} \langle E_{K_n} \rangle. \quad (13)$$

Similarly the correlation $\langle \mathcal{H}_{KL} \mathcal{H}_{MN} \rangle_e = 0$ if $(K, L) \neq (M, N)$; this is again due to presence of both positive as well as negative contributions which on summation cancel each other. Further ignoring the correlations between the matrices \mathcal{H}_0 and \mathcal{U} and using eqs.(8,9), the 2^{nd} moment of \mathcal{H}_{KL} can be approximated as

$$v_{KL} \equiv \langle (\mathcal{H}_{KL})^2 \rangle = \sum_{n=1}^{g_0} \langle E_{K_n}^2 \rangle \delta_{KL} + \langle (\mathcal{U}_{KL})^2 \rangle \quad (14)$$

Squaring \mathcal{U}_{KL} leads to mixed many body terms which can be positive as well as negative and their average over an ensemble leads to negligible contribution. As a consequence, the significant contribution to v_{KL} comes only from the square of many body terms. Further as v_{kl} for a p -plet consists of the many body contributions among p or more molecules, it is relatively weaker for higher-plets (see *appendix F*). The number of p -plets however increases with p , their collective contribution need not be negligible.

D. Non-polar Molecules

The matrix elements and their variance given by eq.(11) and eq.(F3) are valid for both polar as well non-polar molecules. But to gain better insight without loss of generality, henceforth we focus on non-polar molecules. The 2nd term in eq.(11) then consists of dispersion interaction only. Contrary to induction, a n -body dispersion interaction corresponds to n instantaneous dipoles interacting with each other and results in change of the states of all n -molecules. Its contribution to a matrix element in the NIM basis is therefore non-zero only if the pair of basis-states form an n -plet. (The latter refers to a pair of basis states $|\mathcal{K}\rangle, |\mathcal{L}\rangle$ which differ in eigenfunction contributions from n -molecules i.e $\mathcal{K}_m \neq \mathcal{L}_m$ with m taking n -values from the set $\{1, 2, \dots, g_0\}$). Eq.(11) can then be rewritten as $\mathcal{U}_{\mathcal{KL}} = \mathcal{U}_{\mathcal{KL}}^{(q1, q2, \dots, qn)}$ \mathcal{K}, L pair as an n - *plet* i.e $\mathcal{K}_{q1, q2, \dots, qn} \neq \mathcal{L}_{q1, q2, \dots, qn}$. Further eq.(F1) still remains valid i.e $\mathcal{U}_{\mathcal{KK}} \approx \mathcal{U}_{\mathcal{KK}}^{es}$.

For sufficiently large distance, say R between a molecule pair ($R > 10 a_0$ with a_0 as Bohr radius), the n -body term can be well-approximated by a multi-pole expansion in which the leading order term is of type R^{-3n} (arising from n -dipoles interaction) [45]. For qualitative estimates of the energy, it is sufficient to take the first term in the expansion and one can write

$$\mathcal{U}_{\mathcal{KL}}^{(q1, q2, \dots, qn)} \approx \frac{C_{\mathcal{KL}}^{(3n)}}{|\mathbf{r}_{q1} - \mathbf{r}_{q2}|^3 \dots |\mathbf{r}_{qn} - \mathbf{r}_{q1}|^3}. \quad (15)$$

where $C_{\mathcal{KL}}^{(3n)}$ is the coefficient of term corresponding to n -instantaneous dipoles interaction in multi-pole expansion of $\mathcal{U}_{\mathcal{KL}}$. Further $\mathcal{U}_{\mathcal{KK}}^{es}$, the expectation value of the electrostatic energy for the set of g_0 molecules in state \mathcal{K} , can also be represented by a multi-pole expansion; here the leading order term depends on the point symmetry group of the molecules (see section 2.B of [52]). As the static dipole moment of non-polar molecules is zero in the ground state, the leading term comes from the mono-pole-quadrupole moment and is proportional to R^{-3} . In case of neutral molecules, however, the contribution from these terms is zero and one has to consider the next significant term which is quadrupole-quadrupole interaction (R^{-5}) if the quadrupole moment of the molecule is non-zero. Thus assuming that the molecules have zero dipole moment even in the excited states (vibrational), the leading term is proportional to $1/R^5$. For a set of g_0 molecules, the additivity of electrostatic energy then gives $\mathcal{U}_{\mathcal{KK}}^{es}(\mathbf{r}_1, \dots, \mathbf{r}_{g_0}) \approx \sum_{\substack{i, j=1 \\ i > j}}^{g_0} \frac{C_{\mathcal{KK}}^{es}(i, j)}{|\mathbf{r}_i - \mathbf{r}_j|^5}$ where $C_{\mathcal{KK}}^{es}(i, j)$ is the strength of electrostatic

interaction (of quadrupole-quadrupole type) for the molecule pair located at positions $\mathbf{r}_i, \mathbf{r}_j$ and in the state \mathcal{K} (i.e n^{th} molecule in state \mathcal{K}_n for $n = 1 \rightarrow g_0$). The mean values for the quadrupole moment for a range of molecules can be of the order of $1 - 5 \text{ amu}$ ($10^{-40} C - m^2$) (see Table III of [52]) and the contribution from the quadrupole-quadrupole interaction for two isolated molecules at a typical molecular distance of $\sim 5\text{\AA}$ is of the order of $10^{-19} J$. The strength $C_{\mathcal{K}\mathcal{K}}^{es}(i, j)$ however depends on the orientation of the molecular-pair too and can be positive, negative as well as zero (see section 3.4.2 of [45]). The net electrostatic contribution from $g_0(g_0 - 1)/2$ pairs of a cluster of $g_0 \gg 1$ randomly oriented but homogeneously distributed molecules within a basic block is therefore expected to be negligible.

Based on the above, the matrix elements of \mathcal{H} can now be approximated as

$$\mathcal{H}_{\mathcal{K}L} \approx \sum_{n=1}^{g_0} E_{\mathcal{K}_n} \quad \text{for } \mathcal{K} = L \quad (16)$$

$$\approx \frac{C_{\mathcal{K}L}^{(3n)}}{|\mathbf{r}_{q1} - \mathbf{r}_{q2}|^3 \dots |\mathbf{r}_{qn} - \mathbf{r}_{q1}|^3} \quad \text{for } \mathcal{K} \neq L. \quad (17)$$

Similar to $C_{\mathcal{K}\mathcal{K}}^{es}$, the coefficients $C_{\mathcal{K}L}^{(3n)}$ also depend on the mutual orientation of the molecules and, under conditions in which all mutual orientations of the molecules are equally probable, the average of $C_{\mathcal{K}L}^{(3n)}$ over an ensemble of the basic blocks, for a fixed pair of \mathcal{K}, L states, can safely be assumed to be zero. (Note, as mentioned near eq.(15), $C_{\mathcal{K}L}^{(3n)}$ refers to the strength of n -instantaneous dipole interactions in a basic block and is expected to vary rapidly from one replica to the other in an ensemble of such blocks even if one considers same set of n -molecules in each replica block). This implies $\langle \mathcal{U}_{\mathcal{K}L} \rangle \approx \frac{\langle C_{\mathcal{K}L}^{(3n)} \rangle}{|\mathbf{r}_{q1} - \mathbf{r}_{q2}|^3 \dots |\mathbf{r}_{qn} - \mathbf{r}_{q1}|^3} \approx 0$.

Again ignoring the correlations between \mathcal{H}_0 and \mathcal{U} , the 2nd moment $v_{\mathcal{K}L} = \langle (\mathcal{H}_{\mathcal{K}L})^2 \rangle$ becomes

$$v_{\mathcal{K}\mathcal{K}} \approx \sum_{n=1}^{g_0} \langle E_{\mathcal{K}_n}^2 \rangle \approx g_0 \nu_0, \quad (18)$$

$$v_{\mathcal{K}L} \approx \frac{\langle (C_{\mathcal{K}L}^{(3n)})^2 \rangle}{|\mathbf{r}_{q1} - \mathbf{r}_{q2}|^6 \dots |\mathbf{r}_{qn} - \mathbf{r}_{q1}|^6}. \quad n - plet, \mathcal{K}_{q1, q2, \dots, qn} \neq \mathcal{L}_{q1, q2, \dots, qn}. \quad (19)$$

with $\nu_0 = \langle E_{\mathcal{K}_n}^2 \rangle$ as the 2nd moment of the vibrational energy-levels of a single isolated molecule Hamiltonian $\mathcal{H}_0^{(n)}$. It must be noted that $\langle E_{\mathcal{K}_n}^2 \rangle - \langle E_{\mathcal{K}_n} \rangle^2$ corresponds to the square of the natural line-width of a typical vibrational level due to Heisenberg uncertainty and is negligible at very low temperatures; taking the natural line width of a typical vibrational

level $\sim 10^{-11} \text{ cm}^{-1}$ ($\approx 10^{-34} \text{ J}$) gives $\nu_0 \sim (10^{-34})^2 \text{ J}^2$. Taking $g_0 \sim 10$ (see [51, 75]) gives $v_{\mathcal{K}\mathcal{L}} \sim 10^{-67} \text{ J}^2$. Similarly the correlation $\langle \mathcal{H}_{\mathcal{K}\mathcal{L}} \mathcal{H}_{mn} \rangle_e = 0$ if $(k, l) \neq (m, n)$; this is again due to presence of both positive as well as negative contributions which on summation cancel each other.

As the basis pair \mathcal{K}, L refer to the vibrational states of the electronic ground state, the coefficients $C_{\mathcal{K}\mathcal{L}}^{(3n)}$ are expected to be of the same order for all such basis-pairs and can be approximated by their average value over all states. Let us define \mathcal{C}_{3n}^2 as the mean square of the coefficient of the n -dipole interaction, respectively, with averaging over all the states as well over the ensemble (equivalent to averaging over all orientations):

$$\mathcal{C}_{3n}^2 = \frac{1}{N^2} \sum_{\mathcal{K}, L} \langle (C_{\mathcal{K}\mathcal{L}}^{(3n)})^2 \rangle. \quad (20)$$

Fortunately a determination of the density of the states of the basic block requires a knowledge only of $\sum_{\mathcal{L}} v_{\mathcal{K}\mathcal{L}}$ i.e summing it over all N basis states for a fixed \mathcal{K} . Approximating the contributions from all single molecule vibrational states undergoing dipole transition as almost same, the sum can then be rewritten as

$$\sum_{\mathcal{L}=1}^N v_{\mathcal{K}\mathcal{L}} \approx g_0 \nu_0 + \sum_{n=2}^{g_0} \eta^n \mathcal{C}_{3n}^2 \sum_{\substack{q1, \dots, qn=1 \\ q1 \neq q2 \dots \neq qn}}^{g_0} \frac{1}{|\mathbf{r}_{q1} - \mathbf{r}_{q2}|^6 \dots |\mathbf{r}_{qn} - \mathbf{r}_{q1}|^6}. \quad (21)$$

with $\eta = \mathcal{N} - 1$ as the number of allowed dipole transitions among the \mathcal{N} eigenstates of a single molecule from a fixed state \mathcal{K}_q [50]. Eq.(21) can further be simplified as follows: as n - body dipole-dipole interaction contains a factor of r^{-3n} , four body and higher many body terms are expected to be less important. Besides, no more than four atoms can be in mutual contact (see page 14, section 10.2 of [45]). For order of magnitude calculations, therefore, it suffices to keep the contribution from the nearest neighbor molecules (referred by z) only; (note, as VW forces in amorphous systems are inter-cluster forces i.e between primary structures such as rings, chains or layers etc, the nearest neighbours considered above are those present on adjacent primary structures). Also note that the total number of states \mathcal{L} forming a n -plet (defined above eq.(11)) with a given state \mathcal{K} and involving transitions of nearest neighbor molecules only is $z \mathcal{N}^n$. This leads to

$$\sum_{\mathcal{L}=1}^N v_{\mathcal{K}\mathcal{L}} \approx g_0 \nu_0 + \frac{z_{C_1} g_0 \eta^2 \mathcal{C}_6^2}{2 (2R_v)^{12}} + \frac{z_{C_2} g_0 \eta^3 \mathcal{C}_9^2}{2 (2R_v)^{18}} \quad (22)$$

where $2R_v$ is the distance of closest approach between two nearest neighbor molecules interacting by dispersion interaction, z as the number of nearest neighbors of a given molecule

and g_0 as the total number of molecules in the block. Detailed studies of the higher order dispersion coefficient C_{3n} for various molecules indicate their rapid decay with increasing n (e.g see Table 10.1 and section 10.2 of [45]). Taking the typical distances between neighboring molecules of the order of 5\AA , $C_6 \sim 10^{-78} J - m^6$ and $C_9 \sim 10^{-108} J - m^9$; consequently contribution from the terms containing ν_0 and C_9 is negligible as compared to the term with C_6 [54, 55]. For \mathcal{KL} -pairs forming the lower plets e.g 2,3-plets, it is easy to check that $v_{KL} \gg v_{KK}$.

E. Bulk-Spectral Parameter b

Referring the sum in eq.(22) as $\frac{1}{2b^2}$ for later use, it can then be approximated as

$$\frac{1}{2b^2} = \sum_{\mathcal{L}=1}^N v_{KL} \approx \frac{z g_0 \eta^2 C_6^2}{2 (2R_v)^{12}}. \quad (23)$$

As discussed in next section, b appears as a measure of the bulk-spectrum width and plays an important role in our analysis. C_6 can further be written in terms of the Hamaker constant A_H (a constant for materials) i.e $A_H \approx \pi^2 C_6 \rho_n^2$, with ρ_n as the number density of the molecules. Taking $\Omega_{\text{eff}} = \frac{1}{\rho_n}$ as the average volume available to a typical glass molecule, we have

$$\Omega_{\text{eff}} = s_m (R_v + R_m)^3 \approx (1 + y)^3 \Omega_m \quad (24)$$

with Ω_m the molar volume: $\Omega_m = s_m R_m^3$, with s_m as a structure constant e.g. $s_m = 4\pi/3$ assuming a spherical shape for the molecule. Here R_v is half the distance between two nearest neighbor molecules; the 2nd equality in eq.(24) follows by writing $R_v = y R_m$. The above in turn gives

$$C_6 \approx \frac{A_H (\Omega_{\text{eff}})^2}{\pi^2} \approx \frac{s_m^2}{\pi^2} (1 + y)^6 R_m^6 A_H \quad (25)$$

Further as discussed in [75],

$$g_0 = \frac{\Omega_b}{\Omega_{\text{eff}}} \approx \frac{1}{(1 + y)^3} \left(\frac{R_0}{R_m} \right)^3 = \frac{64 y^3}{(1 + y)^3} \quad (26)$$

Based on the stability analysis of amorphous systems structure, z is predicted to be of the order of 3 (for a three dimensional block). Further, the intermolecular interactions being rather weak, they can mix very few single molecule levels. The dipole nature of these

interactions further suggest $\mathcal{N} = 3$ (the number of relevant vibrational energy levels in a molecule); this in turn implies $\eta = 2$. The above on substitution in eq.(23) leads to

$$b \approx \frac{36}{\eta \sqrt{z} g_0 A_H} \frac{y^6}{(1+y)^6} = \frac{9}{4 \sqrt{3} A_H} \left(\frac{y}{1+y} \right)^{9/2} \quad (27)$$

Experimental data of some standard glasses suggest that R_v is typically of the same order as R_m . Hereafter we use $y = \frac{R_v}{R_m} \sim 1$ in our quantitative analysis. Eq.(26) then gives $g_0 = 8$.

Determination of A_H : for materials in which spectral optical properties are not available, two refractive-index based approximation for A_H namely, standard Tabor-Winterton approximation (TWA) and single oscillator approximation (SOA), provide useful estimates [57]. As indicated by previous studies, TWA is more appropriate for low refractive index materials (for $n < 1.8$); A_H in this case is given as (see eq.(11.14) of [56, 57])

$$A_H \approx \frac{3\hbar\nu_e}{16\sqrt{2}} \frac{(n_0^2 - 1)^2}{(n_0^2 + 1)^{3/2}} \quad (28)$$

with n_0 as the refractive index at zero frequency and ν_e as the characteristic absorption frequency in the ultra-violet (also referred as the plasma frequency of the free electron gas, with a typical value is $\nu_e = 3 \times 10^{15}$ for most ceramics). Further n_0 and ν_e in eq.(28) can be obtained by the standard routes (e.g. Cauchy's Plots or other available formulas) [57]: $n^2(\nu) - 1 = \mathcal{G}_{uv} + \frac{\nu_e^2}{\nu^2} (n^2(\nu) - 1)$. For cases, where the frequency-dependence of n is known either as an exact formula (e.g. V52, BALNA, LAT) or available for two or more frequencies (see *appendix B*), we determine ν_e and $n_0 = \sqrt{1 + \mathcal{G}_{uv}}$ by least square fit to plot $(n^2 - 1)$ vs $(n^2 - 1)/\lambda^2$. (Note eq.(28) is applicable for the case for two molecules interacting by VW interaction with vacuum as the intervening medium, with zero frequency contribution neglected; see eq.(11.14) of [56, 57]).

For materials with higher indexes (for $n > 1.8$) however TWA is found to be increasingly poor; instead, the single oscillator approximation (SOA) [57] is closer to the exact values

$$A_H \approx 312 \times 10^{-21} \frac{(n^2 - 1)^{3/2}}{(n^2 + 1)^{3/2}} J \quad (29)$$

with n as the available value of refractive index; for our calculation, we choose $n = n_0$.

Table I displays n_0 values along with ν_e values for the 18 glasses; (although the latter is not used for the higher index cases but is included here for the sake of completeness). The corresponding A_H values obtained by either eq.(28) or eq.(29) are also given the table along with b values from eq.(27).

III. DENSITY OF STATES (DOS)

At very low temperatures, the induced dipole interactions result in excitations among vibrational energy levels of molecules (not strong enough to excite the electronic states and the chemical bonding prevents the rotation of molecules). In this section, we derive the ensemble averaged density of the states which participate in these excitations. We proceed as follows.

The many body density of states $\rho(e) = \sum_n \delta(e - e_n)$ of the Hamiltonian \mathcal{H} (eq.(1)) can be expressed in terms of the standard Green's function formulation: $\rho(e) = -\frac{1}{\pi} \text{Im } G^\dagger(e)$ with $G^\dagger(e) = \lim_{\epsilon \rightarrow 0} G(e + i\epsilon) = \lim_{\epsilon \rightarrow 0} \text{Tr} \frac{1}{\mathcal{H} - e - i\epsilon}$. The ensemble averaged density of states can then be written as [58]

$$\langle \rho(e) \rangle = -\frac{1}{\pi} \lim_{\epsilon \rightarrow 0} \text{Im} \langle G(z) \rangle \quad (30)$$

with z as a complex number: $z = e + i\epsilon$. One can further write $\langle G(z) \rangle$ in terms of the moments $T_n \equiv \langle \text{Tr } \mathcal{H}^n \rangle$:

$$\langle G(z) \rangle = \langle \text{Tr} \frac{1}{\mathcal{H} - z} \rangle = -\frac{1}{z} \sum_{n=0}^{\infty} \frac{1}{z^n} T_n \quad (31)$$

It is easy to calculate the first three moments. As discussed in section II, $\langle \mathcal{H}_{KL} \rangle = 0$, $\langle \mathcal{H}_{KL}^2 \rangle = v_{KL}$ and $\langle \mathcal{H}_{KL} \mathcal{H}_{MN} \rangle = 0$ if $(K, L) \neq (M, N)$ with v_{KL} given by eq.(19). This gives $T_0 = N$, $T_1 = 0$ and

$$T_2 = \sum_{K,L} v_{KL} = \frac{N}{2} b^2 \quad (32)$$

where b is given by eq.(27). To obtain higher order traces, we expand $\text{Tr } \mathcal{H}^m$ in terms of the matrix elements,

$$T_m = \langle \text{Tr } \mathcal{H}^m \rangle = \sum_{K_1, K_2, \dots, K_m} \langle \mathcal{H}_{K_1 K_2} \mathcal{H}_{K_2 K_3} \dots \mathcal{H}_{K_{m-1} K_m} \mathcal{H}_{K_m K_1} \rangle \quad (33)$$

As clear, the trace operation ensures that the terms always have a cyclic appearance. Further in evaluating T_m for $N \rightarrow \infty$, the terms with only pairwise (binary) correlations will be of consequence, their total number being much larger than all other terms. For example, consider the contribution to T_{2n} from the terms consisting of n -products of v_{KL} (i.e of type $v_{K_L1} v_{L_1 L_2} \dots v_{L_{n-1} K}$) with K, L pairs as 2-plets. From eq.(19) and eq.(25), $v_{KL} \sim A_H^2 \sim$

$10^{-38} J$. The contribution to T_{2n} from all terms with n pairwise correlations among 2-plets is then of the order of $N \times \left(\frac{1}{2} \eta^2 g_0(g_0 - 1) 10^{-38}\right)^n J \approx N \times 2^{7n} 10^{-38n} J$ (with $g_0 = 8$ and $\eta = 2$). Similarly the \mathcal{K}, L pairs forming higher order plets also contribute, their weaker individual contribution compensated by higher number of terms. The total number of terms contributing to T_{2n} and forming n -products of $v_{\mathcal{KL}}$ are $N \times \sum_{p_1, \dots, p_n=2}^{g_0} C_{p_k} \eta^{p_k}$. In contrast, the number of terms in T_{2n} with one or more matrix elements appearing repeatedly is relatively much less (e.g. the terms of type $\langle (\mathcal{H}_{\mathcal{KK}})^{2n} \rangle$ are only N), their net contribution is different by an order of magnitude and can be neglected. (Note, with typical molecular vibrational energies $10^{-20} J$ and $g_0 \approx 8$, the upper bound on $\mathcal{H}_{\mathcal{KK}}$ is $10^{-19} J$. This in turn gives $\sum_{\mathcal{K}} (\mathcal{H}_{\mathcal{KK}})^{2n} \sim N \times 10^{-38n} J$). As discussed in *appendix A* in more detail, T_{2n} can then be approximated as

$$T_{2n} \approx \frac{1}{n+1} \binom{2n}{n} \frac{N}{2^n b^{2n}} \quad (34)$$

The terms contributing to T_{2n+1} are of type $(v_{\mathcal{KL}})^{2(n-t)} \langle (\mathcal{H}_{\mathcal{KK}})^{2t+1} \rangle$; their contribution can however be set to zero by an appropriate choice of the origin of single molecular energy scale. This can be explained as follows. As mentioned above, the allowed number of dipole transitions permit only three vibrational states of each molecule to be involved; without loss of generality, these can be referred as $\varepsilon_0 - \Delta\varepsilon, \varepsilon_0, \varepsilon_0 + \Delta\varepsilon$ (with typical values of $\varepsilon_0, \Delta\varepsilon \sim 10^{-20} J$). With $\mathcal{H}_{\mathcal{KK}} = \sum_{n=1}^{g_0} E_{\mathcal{K}_n}$ and each $E_{\mathcal{K}_n}$ allowed to take any of the three values, clearly $\mathcal{H}_{\mathcal{KK}}$ can vary from $g_0(\varepsilon_0 - \Delta\varepsilon) \rightarrow g_0(\varepsilon_0 + \Delta\varepsilon)$. This in turn gives the spectral average $\overline{\mathcal{H}_{\mathcal{KK}}} = \frac{1}{N} \sum_{\mathcal{K}=1}^N \mathcal{H}_{\mathcal{KK}} \approx g_0 \varepsilon_0$ (with all intermediate states being equally probable due to instantaneous nature of the dipole transitions). This also leads to average of $\mathcal{H}_{\mathcal{KK}}$ over an ergodic ensemble of the basic blocks: $\langle \mathcal{H}_{\mathcal{KK}} \rangle = \overline{\mathcal{H}_{\mathcal{KK}}} \approx g_0 \varepsilon_0$. For technical simplification and again without loss of generality, here we set $\varepsilon_0 = 0$ which results in $\langle \mathcal{H}_{\mathcal{KK}} \rangle = 0$. Following same logic, we have $\langle \mathcal{H}_{\mathcal{KK}} \rangle^{2t+1} = 0$ and as a consequence

$$T_{2n+1} \rightarrow 0 \quad (35)$$

Substituting the above results in eq.(31), we get

$$\langle G(z) \rangle \approx -\frac{N}{z} \sum_{n=0}^{\infty} \frac{1}{n+1} \binom{2n}{n} \left(\frac{1}{2 b^2 z^2} \right)^n$$

$$= -Nzb^2 \left[1 - \left(1 - \frac{2}{b^2 z^2} \right)^{1/2} \right] \quad (36)$$

Now substituting $z = e + i\epsilon$, taking the imaginary part of the above, followed by limit $\epsilon \rightarrow 0$ then gives

$$\langle \rho_{bulk}(e) \rangle = \frac{Nb}{2\pi} \sqrt{2 - (be)^2}. \quad (37)$$

As clear from the above, the bulk of the spectrum, with its width as $2\sqrt{2}/b$ and mean level spacing $\Delta_b \approx \frac{\pi\sqrt{2}}{Nb}$, depends on the single parameter i.e the *bulk-spectrum parameter* b given by eq.(27). As b depends on the average properties of the many body inter-molecular interactions, it is not expected to vary much from one system to another. This is also indicated by eq.(27). For later use, we shift the origin of the spectrum to $e = -\sqrt{2}/b$ and redefine $b = b_0\sqrt{2}$ which gives

$$\langle \rho_{bulk}(e) \rangle = \frac{Nb_0}{\pi} \sqrt{b_0 e(2 - b_0 e)} \quad (38)$$

As displayed in table I for 18 non-metallic glasses, $b \sim 10^{17} - 10^{18} J^{-1}$.

Eq.(38) is analogous to the bulk level-density of a Gaussian orthogonal ensemble (GOE) although the derivation given above does not assume any specific distribution of the matrix elements of the Hamiltonian; (a GOE refers to an ensemble of real-symmetric matrices with independent Gaussian distributed matrix elements with zero mean and variance of the diagonal twice that of the off-diagonal) . A same expression was also obtained in [59] for the bulk level density of a sparse random matrix (with its non-zero elements randomly taking values $0, \pm 1$). Indeed the semi-circle behavior of the bulk level density is known to be valid for a wide range of the matrix elements distributions with finite moments, (typical of dense matrices, irrespective of the nature of their randomness) (see section 4.3 of [62] and [60, 63]). As in our case, the number of non-zero off-diagonals ($\approx N \sum_{p=1}^{g_0} {}^{g_0}C_p \eta^p$) is much larger than the diagonals (total N of them), H *effectively* behaves as a dense matrix and a semi-circle behavior of the level density is expected. An alternative reasoning for GOE type density of states can also be given as follows: as both \mathcal{H}_0 and \mathcal{U} consist of the contributions from many independent random terms, the central limit theorem predicts the distribution of their matrix elements to be Gaussian type. With many non-zero off-diagonals, the ensemble of \mathcal{H} matrices behaves *effectively* as a GOE. Following the above reasoning, the ensemble averaged edge level density $\langle \rho_{edge}(e) \rangle$ for \mathcal{H} can be modeled by that of a GOE too. Using a

generic form, one can write

$$\langle \rho_{edge-t}(e) \rangle = \frac{N b_0}{\sqrt{\lambda}} f_t(\lambda b_0 e). \quad (39)$$

with subscript $t = L, U$ denoting lower ($-\infty < x < 0$) and upper edge ($2 < x < \infty$), respectively, and $f_t(x)$ in case of a GOE is

$$f_L(x) \approx x Ai^2(-x) + (Ai'(-x))^2 + \frac{1}{2} Ai(-x) E(-x) \quad (\text{at lower edge}) \quad (40)$$

$$f_U(x) \approx -(x-2) Ai^2(x-2) + (Ai'(x-2))^2 + \frac{1}{2} Ai(x-2) E(x-2) \quad (\text{at upper edge}) \quad (41)$$

with $E(x) \equiv \int_{-\infty}^x Ai(y) dy$, with $Ai(y)$ as the Airy function of the first kind. For later use, it is worth noting that Airy-function asymptotic of eqs.(40,41) leads to a super-exponential form for $f_L(x)$ for $x < 0$ (*appendix B*)

$$f_L(x) \sim \frac{1}{\sqrt{|x|}} e^{-\sqrt{|x|^3}}. \quad (42)$$

and a square-root form for $x \gg 0$,

$$f_L(x) \approx \frac{\sqrt{c_0^2 + x}}{\pi} + \frac{1}{\pi x} \cos\left(\frac{2}{3} x^{3/2}\right). \quad (43)$$

where $c_0 = 0.1865 \pi$. As expected $f(x)$ is non-zero at $x = 0$; (note $f(x) = 0$ would imply a gap at $x = 0$ instead of smooth connection with the bulk density). Substitution of eq.(43) in eq.(39) gives

$$\langle \rho_{edge-l}(e) \rangle \approx \frac{N b_0}{\pi \sqrt{\lambda}} \sqrt{c_0^2 + \lambda b_0 e} \quad (e > 0) \quad (44)$$

Thus, for $e > 0$, the edge behavior smoothly connects with the beginning of bulk of the ensemble averaged level density (see eq.(38) and figure 1).

Contrary to bulk, the edge-density depends on two parameters b and λ ; the latter, governing the decay of density of states in the lower edge, can be referred as the *edge-spectrum parameter*. Here λ is dimensionless and satisfy the requirement that $\langle \rho_{edge}(e) \rangle = \langle \rho_{bulk}(e) \rangle$ near $e \sim e_0$. For the GOE case, we have

$$\lambda = \lambda_0 N^{2/3} = \mathcal{N}^{2g_0/3} \lambda_0 = 3^{16/3} \lambda_0 \quad (45)$$

with λ_0 is a constant: $\lambda_0 \approx \sqrt{2}$. The 2nd equality in the above follows from $\mathcal{N} = 3$ and $g_0 \approx 8$ (see text below eq.(26)). For later use, it is necessary to determine the point, say e_0 , where the edge of the spectrum meets the bulk; as discussed in *appendix B* and also clear from figure 1, the normalization condition $\int_{-\infty}^{\infty} \langle \rho_e \rangle de = N$ gives

$$e_0 \approx \frac{1}{3 b_0 \lambda} \sim 10^{-21} J \quad (46)$$

Following from eq.(42), the rapid decay of density of states for $e < 0$ implies very few levels in the edge region; this can directly be confirmed from eq.(40) which gives their number, say N_{edge} as

$$N_{edge}(e) = \int_{-\infty}^e \langle \rho_{edge-l}(e) \rangle de = \frac{N \mathcal{F}(\lambda b_0 e)}{\sqrt{\lambda^3}} = \frac{\mathcal{F}(\lambda b_0 e)}{\sqrt{\lambda_0^3}}. \quad (47)$$

with $\mathcal{F}(x) = \int_{-\infty}^x dx f_L(x)$. As can be seen from figure 2, \mathcal{F} is maximum at $e = 0$, with $\mathcal{F}(0) \approx 0.16$, and rapidly decays as $|e|$ increases. Clearly most of the contribution to f_0 is coming from the region $x \sim 0$, indicating the presence of almost all levels in the lower edge region very close to $e = 0$. Further the mean level spacing $\Delta(e)$ at an arbitrary energy e in the edge region is

$$\Delta(e) = \frac{1}{\langle \rho_{edge-l} \rangle} \approx \frac{\sqrt{\lambda}}{N b_0 f_L(\lambda b_0 e)}. \quad (48)$$

The above indicates $\Delta(0) \ll \Delta(e_l)$ with $e_l \ll 0$.

IV. HEAT CAPACITY OF THE BASIC BLOCK

Our next step is to calculate the ensemble averaged heat capacity C_v of a basic-block of volume Ω_b , defined as $\langle C_v \rangle = k \beta^2 \frac{\partial^2}{\partial \beta^2} \langle \log Z \rangle$ with Z as its partition function: $Z = \sum_{n=1}^N \exp[-\beta e_n]$. For cases with annealed disorder, $\langle \log Z \rangle$ can be approximated by $\log \langle Z \rangle$. Although disorder in glasses is generally believed to be of quenched type, the belief is based on the experimentally observed long range structural disorder at macroscopic scales. No such evidence is available however in case of nano-size samples. Further as there is ample evidence of thermodynamics in nano-sizes being different from macroscopic sizes [40–43], a quenched behavior in the latter does not imply the same in the former. The nature of disorder is also different in the two cases. In contrast to structural disorder at macroscopic sizes, the disorder in the basic block arises due to rapidly changing orientation of the instantaneous

dipoles and can appropriately be considered as annealed type (with no external impurities but complexity of interactions leading to randomization of dynamics). This in turn gives

$$\langle C_v \rangle = k \beta^2 \frac{\partial^2}{\partial \beta^2} \log \langle Z \rangle \quad (49)$$

With $\rho(e)$ as the density of states $\rho_e(e) = \sum_{n=1}^N \delta(e - e_n)$ of a typical basic block, Z can also be expressed as $Z = \int de \rho_e(e) \exp[-\beta e]$. For energy ranges where level-spacing is very small, $\rho(e)$ can be approximated by a smooth function i.e its spectral average. In the present case, however, the spectrum consists of regions with very large mean level spacing for $e < 0$ and it is appropriate to separate the discrete and continuous parts of Z [70]: $Z = \sum_{n; e_n < 0} \exp[-\beta e_n] + \int_0^\infty de \bar{\rho}_e \exp[-\beta e]$ with $\bar{\rho}_e$ as the spectral averaged density of states. This in turn leads to

$$\langle Z \rangle = \sum_{n; e_n < 0} \langle \exp[-\beta e_n] \rangle + \int de \langle \bar{\rho}_e \rangle \exp[-\beta e] \quad (50)$$

with $\langle \bar{\rho}_e \rangle$ as the level density averaged over the spectrum as well as the ensemble. (Note the first term here is not spectral averaged).

A. Calculation of $\langle Z \rangle$

Due to different functional behavior of the level density in the edge and bulk regions, we divide $\langle Z \rangle$ in four parts corresponding to lower edge ($-\infty < e \leq e_0$), bulk ($e_0 \leq e \leq (2/b) - e_0$) and upper edge ($(2/b) - e_0 < e \leq \infty$) respectively:

$$\langle Z \rangle = \sum_{n; e_n < 0} \langle \exp[-\beta e_n] \rangle + J_L + J_B + J_U \quad (51)$$

where

$$J_L = \int_0^{e_0} de \langle \rho_{edge-l}(e) \rangle \exp(-\beta e) \quad (52)$$

$$J_B = \int_{e_0}^{\frac{2}{b_0} - e_0} de \langle \rho_{bulk}(e) \rangle \exp(-\beta e) \quad (53)$$

$$J_U = \int_{\frac{2}{b_0} - e_0}^\infty de \langle \rho_{edge-u}(e) \rangle \exp(-\beta e) \quad (54)$$

Substituting eq.(44) in eq.(52), one can rewrite it as

$$J_L = \frac{N b_0}{\pi \sqrt{\lambda}} \int_0^{e_0} de \sqrt{c_0^2 + \lambda b_0 e} \exp(-\beta e) \quad (55)$$

$$\approx \frac{N}{\pi} \left(\frac{1}{3\lambda\beta e_0} \right)^{3/2} \left[\gamma \left(\frac{3}{2}, (1+\eta)\beta e_0 \right) - \gamma \left(\frac{3}{2}, \eta\beta e_0 \right) \right] \exp[\eta\beta e_0] \quad (56)$$

where $\eta \approx 1$, $c_0^2 = (0.1865\pi)^2 \approx 1/3$ and $\gamma(a, x)$ is the incomplete Gamma function defined as $\gamma(a, x) = \int_0^x t^{a-1} e^{-t} dt$ with e_0 and λ given by eq.(45), eq.(46) respectively.

Similarly, J_B can be written as (with $\langle \rho_{bulk} \rangle$ given by eq.(38))

$$J_B \approx \frac{N}{\pi} \int_{be_0}^{2-be_0} dx \sqrt{x(2-x)} e^{-\frac{\beta}{b}x} \quad (57)$$

$$= \frac{N}{2\pi} \Phi\left(\frac{3}{2}, 3, -6\lambda\beta e_0\right) - \frac{N\sqrt{2}}{\pi} \left(\frac{1}{3\lambda\beta e_0}\right)^{3/2} \gamma\left(\frac{3}{2}, \beta e_0\right) - \frac{N\sqrt{6\lambda-1}}{9\pi\lambda^2\beta e_0} e^{-6\lambda\beta e_0} \quad (58)$$

with $\Phi(a, b, x)$ as the confluent Hypergeometric function, defined as $\Phi(a, b_0; x) = \int_0^2 dx \sqrt{x(2-x)} e^{-\frac{\beta}{b_0}x}$. Due to presence of the term $e^{-\frac{\beta}{b}x}$ in the integrant, the contribution from the above integral is significant when $\beta e_0 < 1$ (i.e $k_B T > e_0$ or the temperature T is high enough to ensure the thermal perturbation to access the states in the bulk). With $e_0 \approx (3b_0\lambda)^{-1}$, this requires $T > (3k_B b\lambda)^{-1} \sim 75^\circ K$. (with $\lambda \approx 495$, $b \sim 10^{18} J^{-1}$ and $k_b = 1.38 \times 10^{-23} J/K$).

Further J_U can be calculated by substituting eq.(39) with f_U given by eq.(41). As the integration-range now is $2-be_0 < x < \infty$, the level-density decreases faster than exponential in this range and one can write

$$J_U \approx e^{-3\beta e_0} J_L. \quad (59)$$

This leaves the contribution from J_U significant only for large $3\beta e_0 < 1$ or $T > o(10^2) K$.

Substitution of eqs.(56,58,59) in eq.(51) gives the partition function for the basic block

$$\begin{aligned} \langle Z \rangle = & \sum_{n; e_n < 0} \langle \exp[-\beta e_n] \rangle + \frac{N}{\pi} \left(\frac{1}{3\lambda\beta e_0}\right)^{3/2} \left[\gamma\left(\frac{3}{2}, (1+\eta)\beta e_0\right) - \gamma\left(\frac{3}{2}, \eta\beta e_0\right) \right] e^{\eta\beta e_0} + \\ & + \frac{N}{2\pi} \Phi\left(\frac{3}{2}, 3, -6\lambda\beta e_0\right) - \frac{N\sqrt{2}}{\pi} \left(\frac{1}{3\lambda\beta e_0}\right)^{3/2} \gamma\left(\frac{3}{2}, \beta e_0\right) - \frac{N\sqrt{6\lambda-1}}{9\pi\lambda^2\beta e_0} e^{-6\lambda\beta e_0} \quad (60) \end{aligned}$$

A substitution of the above expression in eq.(49) gives, in principle, the specific heat. The above expression can further be simplified by noting that (i) only a single level is present in the tail region $e < 0$ and that too is very close to $e \sim 0$, one can approximate $\sum_{n; e_n < 0} \langle \exp[-\beta e_n] \rangle \approx 1$, (ii) for $x \gg 1$, $\Phi\left(\frac{3}{2}, 3, -x\right) \approx \frac{2}{\sqrt{\pi}} \frac{1}{\sqrt{x^3}}$ and $\gamma\left(\frac{3}{2}, x\right) \approx \Gamma\left(\frac{3}{2}\right) - (x)^{1/2} e^{-x}$. As, in the present work, our interest is in temperature regime $T < 100^\circ K$, this implies $\lambda\beta e_0 \gg 10^2$ (with e_0 given by eq.(46)) and one can then approximate

$$\langle Z \rangle \approx 1 + \frac{N}{\pi} \left(\frac{1}{3\lambda\beta e_0}\right)^{3/2} \left[\gamma\left(\frac{3}{2}, (1+\eta)\beta e_0\right) - \gamma\left(\frac{3}{2}, \eta\beta e_0\right) \right] e^{\eta\beta e_0} \quad (61)$$

For comparison with the experiments however it is helpful to analyze the specific heat in different temperature regimes.

B. $\langle C_v \rangle$ for low temperatures T

Case (a): $\beta e_0 \gg 1$: As $k_b T \ll e_0$ here, the thermal perturbation mixes very few states even

in the lower edge. With $\beta e_0 \gg 1$ in this case, both γ -functions in eq.(61) can be expanded asymptotically as

$$\gamma(a, x) \approx \Gamma(a) - x^{a-1} e^{-x} \sum_{m=0}^{M-1} \frac{(-1)^m \Gamma(1-a+m)}{\Gamma(1-a) x^m} + O(x^M) \quad (62)$$

Following from the above, the 2nd and higher order terms in the series for $\gamma\left(\frac{3}{2}, (1+\eta)\beta e_0\right)$ are smaller than those of $\gamma\left(\frac{3}{2}, \eta\beta e_0\right)$ by an exponential factor and one can approximate $\gamma\left(\frac{3}{2}, (1+\eta)\beta e_0\right) \approx \Gamma(3/2)$. This along with eq.(62) reduces eq.(61) as

$$\langle Z \rangle \approx 1 + \frac{\sqrt{\eta^3}}{\pi \sqrt{27} \lambda_0^3} \sum_{m=0}^{M-1} \frac{(-1)^m \Gamma(m-1/2)}{\Gamma(-1/2) (\eta\beta e_0)^{m+1}} + O((\beta e_0)^M) \quad (63)$$

Substitution of eq.(63) in eq.(49) now leads to,

$$C_v(T) \approx \frac{k_b \sqrt{\eta^3}}{\pi \sqrt{27} \lambda_0^3} \sum_{m=0}^{M-1} \frac{(-1)^m (m+1)(m+2) \Gamma(m-1/2)}{\Gamma(-1/2) (\eta\beta e_0)^{m+1}} + O((\beta e_0)^M) \quad (64)$$

with $\eta \approx 1$, $\lambda_0 \approx \sqrt{2}$, $e_0 \sim 10^{-21} J$. At very low temperatures, the above indicates a linear T -dependence of the leading order term:

$$C_v(T) \approx 0.22 (\lambda b_0) k_b^2 T + 0.37 (\lambda b_0)^2 k_b^3 T^2 - 2.32 (\lambda b_0)^3 k_b^4 T^3 + O(T^4) \quad (65)$$

It must be noted that the result above is based on approximating $\gamma\left(\frac{3}{2}, (1+\eta)\beta e_0\right)$ only by its first term in the series expansion. At very low T however the difference $\gamma\left(\frac{3}{2}, (1+\eta)\beta e_0\right) - \gamma\left(\frac{3}{2}, \eta\beta e_0\right)$ rapidly decreases and the approximation is not very good. As discussed in *appendix E*, a variation of T leads to a transition in the behaviour of the leading order term of $C_v(T)$ from T to $T^{3/2}$ which could well appear as an intermediate power in measurements.

Case (b): $\beta e_0 \ll 1$

In limit $\beta e_0 \ll 1$, eq.(56) can be approximated by the behavior of $\gamma(a, x)$ near $x = 0$:

$$\gamma(a, x) = \sum_{n=0}^{\infty} (-1)^n \frac{x^{a+n}}{n! (a+n)}. \quad (66)$$

Substitution of the above in eq.(61) gives

$$\langle Z \rangle \approx 1 + \frac{\sqrt{2} e^{\eta \beta e_0}}{\pi \sqrt{27} \lambda_0^3} \sum_{m=0}^{M-1} a_m (\beta e_0)^m + O((\beta e_0)^M) \quad (67)$$

with $a_m = \frac{(-1)^m}{m!(m+3/2)} ((1+\eta)^{m+3/2} - \eta^{m+3/2})$. Substitution of the above in eq.(49) then leads to

$$C_v \approx \frac{k_b e^{\eta \beta e_0}}{\pi \sqrt{27} \lambda_0^3} \sum_{m=0}^{M-1} b_m (\beta e_0)^{m-2} + O((\beta e_0)^{(M+1)}) \quad (68)$$

with $b_m = \frac{(-1)^m}{m!} \left[\frac{\eta_0(m+2)}{(m+7/2)} - \frac{2\eta_0(m+1)}{(m+5/2)} + \frac{\eta_0(m)}{(m+3/2)} \right]$ and $\eta_0(m) = 2^{m+3/2} - 1$. The above gives the leading order term decaying as $\frac{1}{T^2}$.

C. Comparison with experiments

Specific heat experiments on a wide range of glasses indicate a super-linear dependence on temperature below $T \leq 1^\circ K$: $c_v \sim T^{1+\varepsilon}$, $\varepsilon \sim 0.1 \rightarrow 0.3$ and a bump in the plot c_v^{total}/T^3 vs T in the region near $T \sim 10^\circ K$. Although the available experimental results are in general applicable for glass solids of macroscopic size, it is tempting to compare them for those of microscopic size too. Previous studies have indicated that the thermal properties of solids at nano scales are in general different from macro scales. More specifically, the specific heat at nano scales is expected to be bigger than that of macro scales [40, 41, 44].

Theoretical results mentioned in previous section are derived for the heat capacity of a basic block of volume Ω_b . The specific heat corresponding to non-phononic contribution can then be given as

$$c_v = \frac{1}{\rho_m \Omega_b} \langle C_v \rangle. \quad (69)$$

with ρ_m as the mass-density of the glass. As discussed in [51, 75], Ω_b can be expressed in terms of the molar mass M of the molecular units participating in dispersion interaction:

$$\Omega_b = \frac{64M}{\rho_m N_a} \quad (70)$$

with N_a as the Avogrado number. The total c_v of the block however consist of the contribution from phonons too:

$$c_v^{total} = c_v + c_v^{ph} \quad (71)$$

where

$$c_v^{ph} = \frac{9R}{M} \left(\frac{T}{T_D} \right)^3 \int_0^{T_D/T} dx \frac{x^4 e^x}{(e^x - 1)^2} \quad (72)$$

$$= \frac{R}{M x_D^3} \left[\frac{12\pi^4}{5} - 9(x_D^4 + 4x_D^3 + 12x_D^2 + 24x_D + 24)e^{-x_D} \right] \quad (73)$$

with $x_D = T/T_D$ and T_d as the Debye temperature and $R = 8.31$ as the gas constant. Contrary to bulk materials, T_D for nano materials can be affected by the size, composition and dimensionality. Experiments indicate T_D decreases with decreasing size [44].

The heat capacity formulation derived in previous section are expressed in terms of the mathematical functions and their correspondence with experimental results is not directly obvious. For numerical analysis and comparison with experiments, it is instructive to directly substitute eq.(60) for the partition function and use computational techniques to obtain c_v^{total} .

Comparison below $T \sim 1^\circ \text{ K}$: Figure 3 displays the comparison of theoretically predicted c_v^{total} for an amorphous SiO_2 basic block along with the experimental data for a macroscopic block taken from figure 6 of [38]. A good agreement is achieved if the Debye temperature T_D is taken much less than that for a macroscopic system. A lower The good agreement clearly indicates that the super-linearity of specific heat in glasses exist even at nano scales.

In connection with the specific heat below 1° K , there have been experimental reports indicating an absence of linear/ super-linear behavior in some types of bulk glass materials which has been attributed to absence of two level tunnelling states [12–17]. Following discussion in previous section, we find that the linear temperature dependence regime of specific heat for the basic blocks depends on the competition between thermal perturbation and the density of states and is sensitive to the edge as well as bulk parameters λ, b ; for the cases in which $\lambda^2 b k_b \ll 1$ it may therefore move to ultra low temperatures.

Comparison above $T \sim 1^\circ \text{ K}$: Figure 4 displays the total specific heat behavior c_v^{total}/T^3 behaviour (obtained from eqs.(60, 49)) along with experimental result for $a - SiO_2$ taken from figure 1 of [38]; the theoretical results, although derived for a basic block, are

almost consistent with experiments on macroscopic sizes of the glass. The bump in heat capacity for the latter, in the temperature regime near $T \sim 6^\circ \text{ K}$, is however replaced by a plateau region. We believe that the small deviation beyond the bump can be corrected by an exact calculation of $\langle Z \rangle$ edge directly using eq.(39) instead of its approximate form; here $T_D = 190^\circ \text{ K}$. Note $T_D \approx 495^\circ \text{ K}$ for the macroscopic sizes of $a - \text{SiO}_2$ [2]).

V. DISCUSSION AND CONCLUSION

In the end, we summarize with our main ideas and results.

As discussed in [51, 75], a range of dispersion forces acting between molecules introduce a natural length scale in an amorphous system leading to emergence of nano-scale sub-structures (referred as basic blocks in the texts) consisting of a few molecules (i.e basic structural units). As emphasized throughout the text, the present work concerns with physics of one such basic block only.

The lack of detailed information due to complicated molecular interactions within a basic block result in appearance of the latter's Hamiltonian as a random matrix, in the product basis of single molecule states. The physical reasoning discussed in section II and ([75]) gives the size of the block of the typical medium range order ($\sim 20 - 30 \text{ \AA}$) where VW forces are known to dominate in amorphous materials. Further the block is shown to contains only 8 molecules, almost all interacting with each other with same strength and homogeneously distributed within a volume of typically 10^4 \AA^3 ; intuitively this is expected to lead to a delocalization of the many-body states of a block Hamiltonian. This along with the statistics of matrix elements discussed in section II and the bulk DOS derived in section III strongly suggests the block Hamiltonian to be well-represented by a Gaussian orthogonal ensemble (GOE) (a standard random matrix ensemble). The agreement in the bulk suggests GOE type behavior in the spectrum edge too. As the density of states for the latter increases super-exponentially, this is consistent with experimental results for many body states (e.g. see [74]) and further lends credence to the above suggestion.

A DOS with semicircle bulk and super-exponential tails for a basic block is precursor of a boson peak in the DOS for a macroscopic block. This can be explained as follows. As confirmed by recent experiments [76, 77], the vibrational density of states (VDOS) $\rho(\omega)$ changes, with increase in frequency ω , from ω^4 (for $\omega < \omega_{bp}$) to ω^2 dependence, (for $\omega > \omega_{bp}$),

with ω_{bp} as a characteristic frequency of the material, referred as the boson peak frequency. (Note the above powers indicate only local frequency-dependence and the exact functional form of $\rho(\omega)$ is more complicated). Here the contribution in the regime $\omega < \omega_{bp}$ is attributed mainly to non-phononic excitations, with phonons dominating the VDOS in the regime $\omega_{bp} < \omega < \omega_{ir}$ with ω_{ir} as the Ioffe-Regel (IR) frequency; the non-phononic contribution to VDOS in the latter regime is $\propto \omega$. In terms of energy $e \propto \omega^2$, this corresponds to a local change of $\rho(e)$ from $e^{3/2}$ -dependence to a constant with increasing e . The analysis in section III indicates a similar behavior for the basic block: following from eq.(42), the leading term for the edge density of states also shows an $e^{3/2}$ -dependence (as can be seen by the local power law analysis $\frac{d \log \rho(e)}{d \log e}$ with $\rho(e) \sim \exp(-|e|^{3/2})$ and the bulk density near the centre of semicircle approaches a constant).

Further, as discussed in detail in [51], a macroscopic sample of an amorphous material can be described as a collection of interacting basic blocks. The typical volume of a basic block of the order of 10^{-23} cm^3 [75], thus implying $\sim 10^{20}$ basic blocks in an experimental sample size of 1 cm^3 . The convolution of basic block Hamiltonians perturbed by a phonon induced coupling of their stress fields leads to a sparse random matrix type structure for the Hamiltonian of the macroscopic sample [51] and its DOS can be derived by convolution of the single block states. A convolution of semicircles can however lead to a Gaussian DOS in the bulk [72] (or a flat DOS e.g as in a semicircle with large radius). Similarly the convolution of the single block edge states is expected to modify the macroscopic edge density. Clearly a semicircle bulk density of states for a nanosize sample does not rule out the existence of a "boson peak" in samples of experimental size. It suggests, instead, a possible role of the phonon mediated coupling among the basic blocks [51] which could lead to a bell-shaped peak. The results obtain in the present study can then be used to determine the form of VDOS of the macroscopic glass solid as well as its specific heat; this will be discussed elsewhere in detail.

An important question discussed extensively in context of boson peak is its location i.e the boson peak frequency. Although the analysis presented here is confined to nanoscales, it strongly suggest the boson peak frequency ω_{bp} to be of the same order as e_0 , this being the edge-bulk meeting point where the DOS behavior changes from $e^{3/2}$ to a constant in e (see also [75] for further discussion).

Based on the DOS formulation for the basic block, we find that its C_v for $T \sim 1^\circ K$

depends on the parameters of three competing energy scales, namely, thermal perturbation kT , the bulk spectrum parameter b and the edge spectral parameter λ . Based on whichever of these parameters dominates the partition function in eq.(51)), the specific heat of the basic block changes from a linear to super-linear temperature dependence. Previously observed in case of macroscopic samples, such a behavior in nano-limits was neither experimentally reported nor theoretically predicted and is a central result of our analysis. To gain a physical insight in the origin of this behavior, it is useful to note that it arises from a \sqrt{e} -dependence of the ensemble averaged DOS near energy $e > 0$ along with a non-zero value at $e = 0$ (as can be seen from eq.(61) along with definition as $\gamma(3/2, x) = \int_0^x \sqrt{t} e^{-\beta t} dt$). This is a reminder of a similar T -dependence in the electronic contribution to specific heat, originating again from a \sqrt{e} -dependence of the average density of states. Notwithstanding the similarity, the technical origin of \sqrt{e} term is very different in the two cases. While in the electronic case, it follows from non-random considerations (simple counting of states), for the block case the randomization of its Hamiltonian leads to a semi-circle density in the bulk with a super-exponentially decaying tail extended to distances of the $o(\lambda)$. Nonetheless this point deserves a deeper consideration especially in view of recent suggestions that the vibrational DOS of the amorphous system is just a modification of that of a crystal, with the BP as the broadened version of Van Hove singularity [78].

The spectrum edge however contains very few levels (just 1 or 2 of them) below $e < 0$, contributes to C_v only at ultra low T and its explicit formulation is not needed for our analysis. Note while the full partition function of the basic block is given by eq.(60), the derivation of C_v in section IV.B is based on $\langle Z \rangle$ approximated by eq.(61). The latter corresponds to the contribution of states only from the edge-bulk boundary region. A square-root energy dependence of DOS in this regions is necessary for a gapless spectrum and is also consistent with the edge DOS for a GOE. (Note a \sqrt{e} -dependence for $e > 0$ in the latter follows from the Airy functions. This is again not surprising as Airy functions are often known to appear at boundary level problems e.g. smooth caustics in various physics domains). As the results derived by the GOE-modelling of the edge spectrum show good agreement with experiments (see figures 3, 4 for two cases and also [51, 75]), this lends further credence to our theoretical approach. Note however the full partition function given by eq.(60) should be used for higher T -calculation of the C_v of a basic block.

In general, based on sparsity of the Hamiltonian of the macro-size sample, its averaged

density of states may vary from one system to other. However, as displayed in Figure 3, our theoretical prediction for C_v (for a single basic block) deviates from the experimental results for SiO_2 (on a macroscopic sample) only in a small range around the bump (also referred as boson peak). Clearly the increased density of states in the bulk due to convolutions seems to affect C_v only near the boson peak.

An important aspect of our analysis is the size of the amorphous system used for specific heat analysis. While previous theories are based on macro-size samples, the analysis here is confined to nano-size. This is relevant in view of the ample evidence often indicating a variation of thermal properties from nano to macro-scales (e.g see [40–44]). Notwithstanding the different scales, it is worth comparing the similarities, differences and advantages of our approach with theories for macroscales. The latter are broadly based on following basic ideas: (i) structural disorder e.g. quasi-localized vibrations or Euclidean random matrices [18, 20, 24], (ii) microscopic disorder in force constants (heterogeneous elasticity theory) [22, 23], (iii) mesoscopic disorder in shear modulus, (iv) models based on structural correlations over distances $10 \rightarrow 20 \text{ \AA}$ (e.g [27–30]), (v) anharmonicities (e.g.[21]).

The experimentally observed bump in specific heat in temperature range $T \sim 5^\circ - 10^\circ K$ is known to be related to the excess density of states in VDOS of amorphous material. A complete theory of specific heat is therefore expected to explain the origin of boson peak. Previous attempts in this context suggest two possible pathways i.e BP either originates from the structural disorder or the short-range order of the glass (the glassy counterpart of the transverse Van Hove singularity in crystal). Recent experiments however have led to contradictory claims e.g. [78–80] and the topic still remains controversial.

Although the basis of our approach is instantaneous orientational disorder at the scale of medium range order, some of our ideas seemingly overlap with previous studies. Similar to our approach, the relevance of MRO scales to explain glass anomalies was also suggested in studies [27–30] but these are mostly based on existence of correlations supported by experimental/ numerical analysis and usually lack mathematical details. As discussed in [75], the MRO scale in our approach has a physical basis, it corresponds to the distances where phonon mediated coupling of the stress fields of two molecules are balanced by dispersion interaction. The heterogeneous elasticity theory [22, 23] predicts, similar to our case, a standard random matrix GOE) type spectral behaviour of the vibrational states [22] and thereby leading to Boson peak and other glass anomalies. But an important difference

between our approach and [22] is as follows: the randomization of vibrational states in the basic block is not caused by microscopic disorder but due to complexity of intermolecular interactions. (Although the latter does lead to instantaneous orientational disorder of the induced dipoles at the MRO scales, it is not a priori obvious whether it can be interpreted same as in [22, 23]). Furthermore the Hamiltonian of the collection of basic blocks, in general, is expected to be a sparse random matrix (with sparsity system dependent) and need not be a standard random matrix taken from a GOE as assumed in [22, 23].

Based on description of glass solid as elastic networks, microscopic disorder appears as a tool in some effective medium theories too, with coordination number z of the network and compressive strain as the key parameters and neglecting large scale fluctuations of z (e.g [25]). A generalization of these theories including weak interactions among contacts was considered in [26]; Although the latter excludes spatial elastic fluctuations, some of its results are similar to [22, 23] which again suggested the irrelevance of structural disorder. As [26] also suggests the roles of VW interactions as well hierarchy of interactions to understand low temperature properties, this is in spirit similar to our approach. (As mentioned in section II, many types of interactions i.e electrostatic and induction (besides dispersion) may influence the b -parameter in case of polar molecules). The results in [26] however are obtained by numerical simulations of macroscopic samples and their quantitative applicability to nano-size sample is not obvious. Further, contrary to our approach, the VW interactions in [26] are assumed to change only the energy-scaling.

Contrary to many previous theories, our theory is neither based on assumed existence of any hypothetical defects nor has any adjustable parameters. The basis of our approach are the basic structural units, interacting by VW interactions within MRO scales and their existence is well-documented in the domain of glass chemistry. The only parameter b that appears in our formulation, depends on the molecular properties e.g. polarisability, ionisation energy, molecule volume and strengths of VW interactions which are experimentally well-measured and a knowledge of their order of magnitudes is sufficient for our purpose; (note λ is a constant). As displayed in table I, $b \sim 10^{18}$ for a wide range of glasses which in turn predicts an analogous behavior of the C_v at low T for them and is consistent with experimental observations for macro-size samples too (notwithstanding the density of states derived here valid only for nano-scales).

Although the derivation of b in section II.E assumes the amorphous molecules to be non-

polar and thus applicable to insulators only, it can directly be extended to polar molecules by including intermolecular interactions of the induction type. Furthermore our approach also suggests a possible explanation of the time-dependence of C_v noted in experiments: it could arise from instantaneous aspect of the dispersion interactions.

A lack of orientational randomization at medium range order in a crystalline material rules out applicability of the theory discussed here to crystals and thereby lack of the universality in the low temperature specific heat. But as the molecules in a crystal are also subjected to VW interactions, it is natural to query as to why the complexity of VW interactions does not lead to randomization in that case? The answer lies in various symmetries of the crystal, resulting in high number of degeneracies among the vibrational energy levels and their clustering, thus ruling out a semicircle density of states (note the latter follows due to repulsion of energy levels) and indicating, instead, a Gaussian density even in a nano-size sample. The observed Boson peaks in crystals may then be explained along the same route.

A complete theory of glass anomalies is expected to explain all universalities of low temperature physical properties. The success of our approach to explain some of them, namely specific heat, ultrasonic attenuation in [51] and Messiner-Berret ratio [75] etc. encourages one to seek its applicability for other anomalies too; we hope to pursue some of them in near future.

Acknowledgments

I am indebted to Professor Anthony Leggett for introducing me to this rich subject and continuous intellectual support in form of many helpful critical comments and insights over a duration of fourteen years in which this idea was pursued. I am also very grateful to Professor Michael Berry for advise in fundamental issues and important technical help in dealing with Airy function integrals which forms the basis of my calculation.

-
- [1] R.C. Zeller and R.O. Pohl, Phys. Rev. B, 4, 2029, (1971).
 - [2] R. B. Stephens, Phys. Rev. B, 8, 2896, (1973).
 - [3] R.O.Pohl, X.Liu and E.Thompson, Rev. Mod. Phys. 74, 991, (2002).
 - [4] P.W. Anderson, B.I. Halperin and C.M. Verma, Philos. Mag. 25, 1, (1972).
 - [5] W.A. Phillips, Two Level States in Glass, rep. Prog. Phys. 50, 1657, (1987); R. Hunklinger and K. Raychandharai, in Progr. Low-Temp. Phys. (ed. D. F. Brewer, Elsevier, Amsterdam), 9, 265, 1986; J. Jackle, *Amorphous Solids: Low-Temperature Properties*, (Springer, Berlin) 1981.
 - [6] Y. M. Galperin, V. G. Karpov and N. Solovjevv, Eksp. Teor. Fiz., 94 (1988) 373.
 - [7] M.A. Ramos, Low Temp. Phys. 46, 104 (2020).
T. Pérez-Castañeda, C. Rodríguez-Tinocob, J. Rodríguez-Viejob and M. A. Ramos, 111, 11275,
 - [8] M. A. Ramos, T. Pérez-Castañeda, R. J. Jiménez-Riobóo, C. Rodríguez-Tinoco, and J. Rodríguez-Viejo, Low Temp. Phys. 41, 412 (2015);
 - [9] A. J. Leggett and D. Vural, J. Phys. Chem. B, 42,117, (2013).
 - [10] A.J. Leggett, Physica B: Cond. Matt. 169, 332 (1991).
 - [11] C.C.Yu and A.J.Leggett, Comments Condens Matter Phys 14, 231, (1988).
 - [12] T. Perez-Castaneda, C. Rodriguez-Tinoco, J. Rodriguez-Viejo and M. A. Ramos, PNAS, 111, 11275, (2014).
 - [13] Xiao Liu, B. E. White, Jr., R. O. Pohl, E. Iwanizcko, K. M. Jones, A. H. Mahan, B. N. Nelson, R. S. Crandall, and S. Veprek, Phys. Rev. Lett., 78, 4418, (1997).
 - [14] B.L. Zink, R. Pietri and F. Hellman, Phys. Rev. Lett., 96, 055902, (2006).
 - [15] D. R. Queen, X. Liu, J. Karel, T.H. Metcalf and F. Hellman, Phys. Rev. Lett., 110, 135901, (2013).
 - [16] N.I. Agladze, A.J. Sivers, Phys. Rev. Lett., 80, 4209, (1998).
 - [17] C. A. Angell, C.T. Moynihan and M. Hemmati, J. Non-Crystalline solids, 274, 319, (2000).
 - [18] V.G.Karpov, M.I.Klinger, F.N.Ignatiev, Sov. Phys. JETP 57, 439, (1983).
 - [19] U. Bucheanau, Y. M. Galperin, V. Gurevich, D. Parashin, M. Ramos and H. Schober, Phys. Rev. B 46, 2798, (1992); 43, 5039, (1991)

- [20] D. A. Parashin, Phys. Rev. B, 49, 9400, (1994).
- [21] V. Gurevich, D. Parashin and H. Schrober, Phys. Rev. B, 67, 094203, (2003).
- [22] W. Schirmacher, G. Diezemann and Carl Ganter, Phys. Rev. Lett., 81, 136, (1998); W. Schirmacher, Euro. Phys. Lett., 73, 892, (2006).
- [23] A. Maruzzo, W. Schirmacher, A. Fratalocchi and G. Ruocco, Sci. Rep., 3, 1407, (2013).
- [24] T. Grigera, V. Martin-Mayor, G. Parisi and P. Verrocchio, Nature, 422, 289, (2003).
- [25] M. Wyart, Euro. Phys. Lett., 89, 64001, (2010).
- [26] E. DeGiuli, A. Laversanne-Finot, G. During, E. Lerner and M. Wyart, Soft Matter, 10, 5628, (2014).
- [27] S.R.Elliott, Europhys. Lett. 19, 201 (1992).
- [28] E. Duval, A. Boukenter, T. Achibat, J. Phys. Condens. Matter 2, 10227, (1990).
- [29] V. K. Malinovsky, V. N. Novikov, P.P. Parashin, A.P. Solokov and M.G. Zemlyanov, Europhys. Lett., 11, 43 (1990).
- [30] G. Monaco and V. M. Giordano, PNAS.0808965106.
- [31] C.C.Yu, Phys. Rev. Lett., 63, 1160, (1989).
- [32] D. Vural and A.J.Leggett, J. Non crystalline solids, 357, 19, 3528, (2011).
- [33] V. Lubchenko and P. G. Wolynes, Phys. Rev. Lett. 87, 195901, (2001).
- [34] M. Turlakov, Phys. Rev. Lett., 93, 035501, (2004).
- [35] A.L. Burin, J. Low. Temp. Phys. 100, 309 (1995); A.L.Burin and Y.Kagan, Physics Letters A, 215 (3-4), 191, (1996).
- [36] J. P. Sethna and K.S. Chow, Phase Tans. 5, 317 (1985); M. P. Solf and M.W.Klein, Phys. Rev. B 49, 12703 (1994).
- [37] M. Baggioli and A. Zaccane, Phys. Rev. Research 1, 012010(R), (2020); M. Baggioli, R. Milkus, and A. Zaccane, Phys. Rev. E 100, 062131, (2019).
- [38] J.C. Phillips, J. Non-crys. solids 43, 37, (1981); 34, 153, (1979).
- [39] S.R.Elliott, Nature, 354, 445, (1991).
- [40] L. Qiu, N. Zhu, Y. Feng, E. E. Michaelides, G. Żyła, D. Jing, X. Zhang, P. M. Norris, C. N. Markides, O. Mahian, Physics Reports 843, 1, (2020).
- [41] Y. D. Qu, X. L. Liang, X. Q. Kong, and W. J. Zhang, Physics of Metals and Metallography,(Pleiades Publishing Ltd.), 118, 528, (2017).
- [42] M. Hartmann, G. Mahler and O.Hess, arXiv:quant-ph/0312214v4.

- [43] G. Guisbiers and L. Buchaillot, Physics Letters A 374, 305, (2009).
- [44] Yan-Li Ma, Ke Zhu and Ming Li, Phys.Chem.Chem.Phys., 20, 27539, (2018); M. Singh, S. Lara and S. Tlali, Jou. Taibah University for Science 11 (2017) 922–929; N. Arora, D. P. Joshi, U. Pachauri, Materials Today: Proceedings 4 (2017) 10450–10454;
- [45] A.J.Stone, *The theory of intermolecular forces*, Oxford scholarship online, Oxford university Press, U.K. 2015.
- [46] H. Y. Kim, J. O. Sofod, D. Velegol, M. W. Cole, and A. A. Lucas, J. Chem. Phys. 124, 074504.190, (2006).
- [47] The NIM basis can be truncated for the following reason. The typical energy of excitation for electronic, vibrational and rotational level in molecules is of the order of $10^{-19} J, 10^{-20} J, 10^{-23} J$ respectively. The thermal perturbation at very low temperatures ($T < 30K$) is not strong enough to result in the electronic state excitations and the molecule remain in its electronic ground state. It could however cause transitions to its roto-vibrational excited states.
- [48] M. Schechter and P.C.E. stamp, arXiv: 0910.1283, (2009); A. Gaita-Ariño and M. Schechter, Phys. Rev. Lett. 107, 105504, (2011).
- [49] Th. Zimmerman, H. Koppel, L. S. Cederbaum, G. Persch and W. Demtröder, Phys. Rev. Lett. 61 3, (1988).
- [50] Here $(C_{KL}^{(3n)})^2$ is first replaced by \mathcal{C}_{3n}^2 which then permits the replacement of the sum $\sum_{\mathcal{L}=1}^N$ by the equivalent sums $\sum_{n=2}^{g_0} \sum_{\substack{q_1, \dots, q_n=1 \\ q_1 \neq q_2 \dots \neq q_n}}^{g_0}$; the latter sum here corresponds to, for a given n , to all n -molecules which undergo transition from their respective single-particle states in \mathcal{K} to those in \mathcal{L} .
- [51] P. Shukla, arXiv:2009.00556.
- [52] I.G.Kaplan and O.B. Rodimova, Sov. Phys. Usp. 21(11), 1978.
- [53] A.D.Buckingham, Adv. Chem. Phys. 12, 107, (1967).
- [54] For qualitative analysis, \mathcal{C}_6 can be approximated by London’s formula $\mathcal{C}_6 \approx \frac{3}{2}\alpha^2 I$ with α as the molecular polarizability averaged over all orientations and I as the first ionization potential [45, 52, 55, 56]). (As mentioned in chapter 6 of [45], α is roughly proportional to molecular volume and ionization potentials do not differ much among different molecules). Similarly $\mathcal{C}_9 \approx 3/4\alpha \mathcal{C}_6$ (applying eq.(10.2.5) of [45] for identical molecules). Taking typical values of the molecular polarizability $\alpha \sim 10^{-30} m^3$ and $I \sim 10^{-18} J$, gives $\mathcal{C}_6 \sim 10^{-78} J - m^6$ and

$$C_9 \sim 10^{-108} J - m^9.$$

- [55] Although more exact expressions for C_6 and C_9 are also available e.g see chapter 4 of [45]) or eq.(2.34) to eq.(2.40) of [52] but London's formula gives fairly accurate values for interactions in a vacuum. These values are usually lower than more rigorously determined ones.
- [56] J. Israelachvili, Chapter 11, *Intermolecular and Surface Forces*, 3rd ed. Academic Press, (2011).
- [57] R.H. French, J. Am. Ceram. Soc., 83, 2117, (2000).
- [58] H-J Stockmann, **Quantum Chaos: an introduction**, Cambridge univ. Press (1999) (see page 79).
- [59] G. J. Rodgers and A. J. Bray, Phys. Rev. B, 37, 3557, (1998).
- [60] A. Khorunzhy and G. J. Rodgers, J. Math. Phys. 38, 3300 (1997).
- [61] T. Guhr, G. A. Muller-Groeling and H. A. Weidenmuller, Phys. Rep. 299, 189 (1998).
- [62] M.L.Mehta,*Random Matrices*, Academic Press, (1991).
- [63] R.C Jones, J M Kosterlitz and D J Thouless, J. Phys. A: Math. Gen., 11, 3,1978.
- [64] D. Turnbull and D. E. Polk, J. Non-crys. solids 8, 19, (1972).
- [65] C. Buchner, L. Lichenstein, H.-J. Freund, *noncontact atomic force microscopy, nanoscience technology*, S. Moira et. al. (eds.), Springer int. Pub. 2015, DOI. 10.11007/978 - 3 - 319 - 15588 - 3₁₆.
- [66] D.Ma, A.D.Stoica and X.-L. Wang, Nature Material 8, 30, (2009).
- [67] R.H.French, R.M.Cannon, L.K.DeNoyer and Y.-M. Chiang, Solid State Ionics, 75, 13, (1995);
- [68] L. Zhang, F. Gan and P. Wang, Applied Optics, 33, 50, (1994).
- [69] M.J. Weber, **Handbook of optical materials**, CRC Press (U.S.A), (2003).
- [70] In case of the standard formulation for the partition function, (with ground state assumed to be at $e = 0$), the lower and upper limits are $e = 0$ and ∞ , respectively. To avoid divergence of the integral at negative energies, extra care for the lower limit must be taken for the cases where the ground state occurs at $e < 0$. Following from eq.(40), although the theoretical form of the density of states in our case extends to $e \rightarrow -\infty$, however as discussed in section III, very few i.e 1 - 2 levels exist in the region $e \sim 0$ even in large N limit (with N as size of the spectrum). Using a continuous form of the $\rho(e)$ is therefore not justified in this region and can introduce errors in the calculation.
- [71] G.H. Abbady, K. A. Aly , Y. Saddeek and N. Affify, Bull. Mater. Sci., Indian Academy of

- Sciences, 1819, (2016); (DOI 10.1007/s12034-016-1328-239).
- [72] T.A.Brody, J.Flores, J.B.French, P.A.Mello, A. Pandey and S.S.M Wong, Rev. Mod. Phys., Vol. 53, No. 3, July 1981.
 - [73] J.F. Berret and M. Meissner, Z. Phys. B-Condensed Matter 70, 65, (1988).
 - [74] M. G. Vavilov, P. W. Brouwer, V. Ambegaokar, and C. W. J. Beenakker Phys. Rev. Lett. 86, 874, (2001).
 - [75] P.Shukla, to be submitted.
 - [76] E. Lerner, G. Düring, and E. Bouchbinder, Phys. Rev. Lett., 117, 035501, (2016).
 - [77] H. Mizuno, H. Shiba and A. Ikeda, PNAS 114, E9767, (2017).
 - [78] A. I. Chumakov et al., Phys. Rev. Lett. 106, 225501 (2011).
 - [79] Y. Wang, L. Hong, Y. Wang, W. Schirmacher and J. Zhang, Phys. Rev. B 98, 174207 (2018).
 - [80] Y. Nie, H. Tong, J. Liu, M. Zu, N. Xu, Front. Phys. 12, 126301 (2017)

TABLE I: **Specific heat calculation: relevant data for 18 glasses:** here the columns 3, 4 give the mass density ρ_m of the glass and the molar mass M of the relevant unit undergoing dispersion interaction (see [51] for details), respectively. This data is used in eq.(70) to obtain the volume of the basic block, displayed in column 5. The columns 6, 7, 8, 9 display the optical parameters for the glass, namely refractive index n_I , characteristic frequency ν_e , Hamaker constant A_H and edge-spectral parameter b (see eq.(27) and eq.(28,29) and *appendix c*); note A_H corresponds to non-retarded dispersion interaction (see eq.(11.14) of [56] or eq.(13b) of [67] with medium 2 as vacuum). From eq.(65), the specific heat for very low T can be expressed as $c_v = c_1 T + o(T^2)$; c_1 values for 18 glasses are given in column 10, along with available ones from [2].

Index	Glass	ρ_m	M	Ω_b	n_I	ν_e	A_H	b	c_1	$c_{1,stephen}$
Units		$\times 10^3 \frac{Kg}{m^3}$	$\frac{gm}{mole}$	10^4 angstroms^3		$\times 10^{15} \text{ sec}^{-1}$	$\times 10^{-20} J$	$\times 10^{18} J^{-1}$	$\frac{ergs}{gm-K^2}$	$\frac{ergs}{gm-K^2}$
1	a-SiO2	2.20	120.09	5.80	1.45	3.24	6.31	0.91	10	11
2	BK7	2.51	92.81	3.93	1.51	3.10	7.40	0.78	12	
3	As2S3	3.20	32.10	1.07	2.35	1.41	17.98	0.32	14	14
4	LASF	5.79	167.95	3.08	1.80	3.00	15.15	0.38	3	
5	SF4	4.78	136.17	3.03	1.72	1.98	8.40	0.68	7	
6	SF59	6.26	92.81	1.58	1.89	1.70	13.12	0.44	7	
7	V52	4.80	167.21	3.70	1.51	3.40	8.37	0.69	6	
8	BALNA	4.28	167.21	4.15	1.47	3.24	6.87	0.84	7	
9	LAT	5.25	205.21	4.15	1.51	3.79	9.16	0.63	4	
10	a-Se	4.30	78.96	1.95	1.90	2.56	13.34	0.43	8	7.5
11	Se75Ge25	4.35	77.38	1.89	3.64	0.68	24.88	0.23	4	
12	Se60Ge40	4.25	76.43	1.91	4.65	0.48	27.15	0.21	4	
13	LiCl:7H2O	1.20	131.32	11.63	1.39	3.19	4.75	1.21	13	
14	Zn-Glass	4.24	103.41	2.59	1.53	3.00	7.71	0.74	10	
15	PMMA	1.18	102.78	9.26	1.48	2.82	6.10	0.94	13	46
16	PS	1.05	27.00	2.73	1.56	2.15	6.03	0.95	49	51
17	PC	1.20	77.10	6.83	1.56	2.08	6.00	0.96	17	38
18	Epoxy	1.20	77.10	6.83	1.54	1.84	4.91	1.17	21	

Appendix A: Derivation of eq.(34)

To obtain higher order traces, we expand $\text{Tr } \mathcal{H}^n$ in terms of the matrix elements,

$$\text{Tr } \mathcal{H}^n = \sum_{\mathcal{K}_1, \mathcal{K}_2, \dots, \mathcal{K}_n} \mathcal{H}_{\mathcal{K}_1 \mathcal{K}_2} \mathcal{H}_{\mathcal{K}_2 \mathcal{K}_3} \dots \mathcal{H}_{\mathcal{K}_{n-1} \mathcal{K}_n} \mathcal{H}_{\mathcal{K}_n \mathcal{K}_1} \quad (\text{A1})$$

As clear, the trace operation ensures that the terms always have a cyclic appearance.

Let us first consider even order Traces. Using $n = 2$ in eq.(A1), T_4 can be written as

$$T_4 = \langle \text{Tr } \mathcal{H}^4 \rangle = \sum_{\mathcal{K}, J, L, M} \langle \mathcal{H}_{\mathcal{K}J} \mathcal{H}_{JL} \mathcal{H}_{LM} \mathcal{H}_{MK} \rangle \quad (\text{A2})$$

Again, due to zero mean of the off-diagonal matrix elements and a lack of correlations among them, the surviving terms in this case are the following: (i) $\sum_{\mathcal{K}, J, M} \langle \mathcal{H}_{\mathcal{K}J} \mathcal{H}_{JK} \mathcal{H}_{KM} \mathcal{H}_{MK} \rangle$, (ii) $\sum_{\mathcal{K}, J, L} \langle \mathcal{H}_{\mathcal{K}J} \mathcal{H}_{JL} \mathcal{H}_{LJ} \mathcal{H}_{JK} \rangle$, (iii) $\sum_{\mathcal{K}, J} \langle \mathcal{H}_{\mathcal{K}J}^4 \rangle$, (iv) $\sum_{\mathcal{K}} \langle (\mathcal{H}_{\mathcal{K}\mathcal{K}})^4 \rangle$. To proceed further, we note that the sum containing the same matrix element repeatedly are of the lower order in g_0 than the sums with pairs. This can be explained as follows: the terms of type (i, ii, iii) contain contributions from n -plet, $n = 1 \rightarrow g_0$, with lower-plets dominating the higher-plets in strength but latter being more in number their total contribution may not be negligible. Considering only the 2-plets, their numbers in the sums of types (i, ii, iii) are $O(Ng_0^4\eta^4)$, $O(Ng_0^4\eta^4)$, $O(Ng_0^2\eta^2)$. Clearly, with $g_0 = 8$ and $\eta = 2$, the sum of type (i, ii) dominate over (iii) even if one considers the contribution from 2-plets and ignores the higher ones. Proceeding similarly it can be seen that the higher order plets contributing to sum in type (i, ii) are much larger in number relative to sum in type (iii). Further the sum in type (iv) is much smaller than (i, ii, iii); this follows because the number of terms in type (iv) are $O(N)$ and an off-diagonal matrix element forming a lower-plet is stronger than a typical diagonal. In large N -limit, therefore T_4 is dominated by the terms with pairwise-correlations and can be approximated as

$$T_4 \approx \sum_{\mathcal{K}, J} v_{\mathcal{K}J} \langle (\mathcal{H}^2)_{\mathcal{K}\mathcal{K}} \rangle + \sum_{\mathcal{K}, J} v_{\mathcal{K}J} \langle (\mathcal{H}^2)_{JJ} \rangle \quad (\text{A3})$$

But as

$$\langle (\mathcal{H}^2)_{\mathcal{K}L} \rangle = \sum_{\mathcal{M}} \langle \mathcal{H}_{\mathcal{K}\mathcal{M}} \mathcal{H}_{\mathcal{L}\mathcal{M}} \rangle = \delta_{\mathcal{K}L} \sum_{\mathcal{M}} v_{\mathcal{K}\mathcal{M}}, \quad (\text{A4})$$

eq.(A3) can be rewritten as

$$T_4 \approx \sum_{\mathcal{K}, J, L} v_{\mathcal{K}J} v_{\mathcal{K}L} + \sum_{\mathcal{K}, J, L} v_{\mathcal{K}J} v_{JL} = 2 \sum_{\mathcal{K}} \left(\sum_{\mathcal{J}} v_{\mathcal{K}J} \right)^2 = \frac{N}{2b^4} \quad (\text{A5})$$

where the last step follows from eq.(27). Similarly, we have

$$\begin{aligned} T_6 &\approx 2 \sum_{\mathcal{K}, J} v_{\mathcal{K}J} \langle (\mathcal{H}^4)_{\mathcal{K}K} \rangle + \sum_{\mathcal{K}, J} v_{\mathcal{K}J} \langle (\mathcal{H}^2)_{\mathcal{J}J} \rangle \langle (\mathcal{H}^2)_{\mathcal{K}K} \rangle \\ &= 4 \sum_{\mathcal{K}, J, L} v_{\mathcal{K}J} \langle (\mathcal{H}^2)_{\mathcal{K}L} \rangle \langle (\mathcal{H}^2)_{\mathcal{L}K} \rangle + \sum_{\mathcal{K}, J, L, M} v_{\mathcal{K}J} v_{\mathcal{J}L} v_{\mathcal{K}M} \end{aligned} \quad (\text{A6})$$

Further using eq.(A4), we get

$$T_6 = 5 \sum_{\mathcal{K}, J, M, S} v_{\mathcal{K}J} v_{\mathcal{K}M} v_{\mathcal{K}S} = 5 \sum_{\mathcal{K}} \left(\sum_{\mathcal{J}} v_{\mathcal{K}J} \right)^3 = \frac{5N}{8b^6} \quad (\text{A7})$$

We now proceed to calculate T_{2n} directly:

$$T_{2n} = \sum_{\mathcal{K}} \langle (\mathcal{H}^{2n})_{\mathcal{K}K} \rangle = \sum_{\mathcal{K}, L} \langle \mathcal{H}_{\mathcal{K}L} (\mathcal{H}^{2n-1})_{\mathcal{L}K} \rangle \quad (\text{A8})$$

For a given term to survive the averaging, one of the factors of \mathcal{H}^{2n-1} must be identical with $\mathcal{H}_{\mathcal{L}K}$. As each one of the $(2n-1)$ factors can play that role, we have $T_{2n} = \sum_{s=0}^{n-1} \sum_{\mathcal{K}, J} \langle \mathcal{H}_{\mathcal{K}J} (\mathcal{H}^{2s})_{\mathcal{J}J} \mathcal{H}_{\mathcal{J}K} (\mathcal{H}^{2n-2s-2})_{\mathcal{K}K} \rangle = \sum_{s=0}^{n-1} \sum_{\mathcal{K}, J} \langle \mathcal{H}_{\mathcal{K}J}^2 \rangle \langle (\mathcal{H}^{2s})_{\mathcal{J}J} \rangle \langle (\mathcal{H}^{2(n-s-1)})_{\mathcal{K}K} \rangle$ which can be rewritten as

$$T_{2n} = \sum_{s=0}^{n-1} \sum_{\mathcal{K}, J} v_{\mathcal{K}J} \langle (\mathcal{H}^{2s})_{\mathcal{J}J} \rangle \langle (\mathcal{H}^{2(n-s-1)})_{\mathcal{K}K} \rangle \quad (\text{A9})$$

Proceeding similarly as for T_4 and T_6 , one can show that $T_{2n} \approx \frac{1}{n+1} \binom{2n}{n} \frac{N}{2^n b^{2n}}$.

Next we consider odd ordered traces. Taking $n = 3$, eq.(A1) gives $T_3 = \langle \text{Tr } \mathcal{H}^3 \rangle = \sum_{\mathcal{K}, J, L} \langle \mathcal{H}_{\mathcal{K}J} \mathcal{H}_{\mathcal{J}L} \mathcal{H}_{\mathcal{L}K} \rangle$. Clearly it contains (i) the terms of type $\langle \mathcal{H}_{\mathcal{K}J} \mathcal{H}_{\mathcal{J}L} \mathcal{H}_{\mathcal{L}K} \rangle$ for $\mathcal{K} \neq J \neq L$, (ii) the terms of type $\mathcal{L} = K \neq J$ or $\mathcal{L} = J \neq K$ or $\mathcal{K} = J \neq L$. (iii) the terms of type $\mathcal{L} = K = J$. As $\langle \mathcal{H}_{\mathcal{K}L} \rangle = a_{\mathcal{K}} \delta_{\mathcal{K}L}$ and different matrix elements are uncorrelated, a term of type (i) or (ii) can contribute only if all matrix elements appearing in it are paired. As the latter is ruled out due to odd number of elements, the contribution from the terms of type (i) or (ii) is zero. The contribution from the terms of type (iii) is however non-zero and this gives

$$T_3 \approx \sum_{\mathcal{K}} \langle (\mathcal{H}_{\mathcal{K}K})^3 \rangle \rightarrow 0 \quad (\text{A10})$$

where the last result follows due to rapid decay of odd-order moments of $\mathcal{H}_{\mathcal{K}K}$ which can be seen from eq.(16) (following the same logic as given in the paragraph above eq.(35)). Further, as in the case of T_3 , all odd ordered traces contain at least one unpaired term which leads to $T_{2n+1} \rightarrow 0$.

Appendix B: Finding e_0 where edge meets bulk

With bulk and the edge level densities given by eq.(38) and eq.(39) respectively, the form of the edge level density is different from that of bulk and it is important to know how and where they connect. Let the edge meet the bulk near $e = e_0$ with e_0 very small, but positive energy. The latter is needed to ensure a gapless spectrum because the bulk density is zero at $e = 0$ but edge-density is not. As mentioned in section III, the point e_0 where edge behavior smoothly joins the bulk behavior can be given by the requirement that

$$\langle \rho_{edge-l}(e_0) \rangle = \langle \rho_{bulk}(e_0) \rangle \quad (B1)$$

Using the large x behavior of Airy functions i.e $Ai(-x) \sim \frac{1}{\pi^{1/2} x^{1/4}} \cos\left(\frac{2}{3} x^{3/2} - \frac{\pi}{4}\right)$, $Ai'(-x) \sim \frac{x^{1/4}}{\pi^{1/2}} \sin\left(\frac{2}{3} x^{3/2} - \frac{\pi}{4}\right)$, $\int Ai(-x) dx \sim \frac{1}{2\pi^{1/2} x^{3/4}} \cos\left(\frac{2}{3} x^{3/2} + \frac{\pi}{4}\right)$, it is easy to show that

$$f(x) \approx \frac{1}{\pi} \sqrt{c_0^2 + x} + \frac{1}{\pi x} \cos\left(\frac{2}{3} x^{3/2}\right). \quad (B2)$$

The above gives $\langle \rho_{edge-l}(e) \rangle \approx \frac{\xi b_0}{\pi} \sqrt{c_0^2 + \lambda b_0 e}$ for $e > 0$. Our next step is to figure out what is ξ and λ ? For this we note that the functional form of both $\rho_{bulk}(e)$ and $\rho_{edge-l}(e)$ should match near $e \sim e_0$.

Substitution of the latter along with eq.(38) in eq.(B1) gives

$$\xi \sqrt{c_0^2 + \lambda b_0 e_0} = \sqrt{2b_0 e_0} \quad (B3)$$

Using $\xi\sqrt{\lambda} = 1$ and $c_0^2 = 1/3$ in the above, we have

$$e_0 = \frac{c_0^2}{b_0 \lambda} \approx \frac{1}{3b_0 \lambda} \quad (B4)$$

To find out exactly the point e_0 i.e where $f(x)$ in eq.(40) begins to behave as a square-root, we take help of Mathematica which gives $\lambda b e_0 \approx 3$ and therefore (See also figure 1)

$$e_0 \approx \frac{1}{3\lambda b_0}. \quad (B5)$$

Appendix C: Calculation of J_B

Using eq.(38), the integral J_B can be written as

$$J_B = \frac{1}{\pi} \int_{b_0 e_0}^{2-b_0 e_0} dx \sqrt{x(2-x)} e^{-\frac{\beta}{b_0} x} \quad (C1)$$

where $e_0 \approx \frac{3}{\lambda b_0}$ (as given by eq.(46)). As an exact evaluation of the above integral in terms of known functions is not available, we need to consider approximations. The exponential is the dominating term in the above integral and therefore dictates the approximation. By rearranging the integral limits, eq.(C1) can be rewritten as

$$J_B = \frac{1}{2\pi} \Phi\left(\frac{3}{2}, 3, -\frac{2\beta}{b_0}\right) - \frac{1}{\pi} I_B \quad (\text{C2})$$

where $\Phi(a, b; x)$ is a confluent Hypergeometric function (defined below eq.(58)) and $I_B = \int_0^{b_0 e_0} dx \sqrt{x(2-x)} \left(e^{-\frac{\beta x}{b_0}} - e^{-\frac{\beta}{b_0}(2-x)} \right)$. Noting that the upper integration limit is $b_0 e_0 \sim 3/\lambda$ with $\lambda \gg 1$, one can approximate $2 - b_0 e_0 \approx 2$ which leads to

$$I_B \approx \sqrt{2} \left(\frac{b}{\beta}\right)^{3/2} \gamma\left(\frac{3}{2}, \beta e_0\right) - \frac{\sqrt{6\lambda - 1}}{9\pi\lambda^2\beta e_0} e^{-6\lambda\beta e_0} \quad (\text{C3})$$

Appendix D: Refractive indices of 18 Glasses

:

As mentioned near eq.(28), the zero frequency refractive index n_0 and characteristic frequency ν for low index material can be determined from the following equation

$$n(\nu)^2 - 1 = \mathcal{G}_{UV} + \frac{\nu^2}{\nu_e^2} (n(\nu)^2 - 1) \quad (\text{D1})$$

For cases where the refractive index for many wavelengths are available, least square fit to plot $(n^2 - 1)$ vs $(n^2 - 1)/\lambda^2$ can be used to extract the slope and intercept. The available data for $n(\lambda)$ however varies from one glass to another. For example, in case of fluoride glasses, $n(\lambda)$ vs λ dependence can be obtained from following relation from [68]

$$n(\lambda)^2 = 1 + \sum_{k=1}^6 \frac{f_k \lambda^2}{(\lambda^2 - \lambda_k^2)} \quad (\text{D2})$$

with λ_k as the wavelengths in ultraviolet (for $k = 1, 2, 3$) and infra-red regime (for $k = 4, 5, 6$), with f_k as the corresponding oscillator strengths; their values are obtained following the steps given in [68]) and displayed in table IV.

For other glasses however $n(\lambda)$ is available only for few wavelengths and is given in tables V, VI. In case of *Zn - glass*, we could find the refractive index of one of its components, namely, *NaPo₃* only for one wavelength; the refractive index for the glass was then obtained by using the standard relation for glass-ceramics i.e $n =$

$\sum_k w_k n_k \rho M_k / \rho_k M$, with w_k as the weight fraction of the component, ρ_k as the mass density, M_k as the molar volume, n_k as its refractive index in the glass; using $(n, w, \rho, M) = (1.547, 0.6, 4.95, 129.2280)$, $(1.4746, 0.2, 4.893, 175.3238)$ and $1.4037, 0.2, 2.181, 101.9617$ for $ZnF_2, BaF_2, NaPO_3$ respectively, with refractive indices for components given at $\lambda = 5876 \text{ \AA}$ [69]. Substitution of these values in the above formula then gives $n = 1.5281$ for Zn-Glass; its A_H was then obtained from eq.(28) (due to lack of information for its characteristic frequency).

TABLE II: Data for eq.(D2) for Floride-glassess (all wavelength are in μm) [68]

Glass	λ_1, f_1	λ_2, f_2	λ_3, f_3	λ_4, f_4	λ_5, f_5	λ_6, f_6
Lat	0.0735, 1.2429	0.1050, 1.3855	0.0828, 1.3044	17.5479, 1.4821	44.4379, 2.7631	25.2953, 1.7069
BALNA	0.07345, 0.6746	0, 0	0.1105, 0.494	17.4112, 0.8214	0, 0	42.6812, 1.7876
LAT	0.0735, 0.7457	0.084, 0.5341	0, 0	17.5479, 0.8893	26.1515, 0.8034	0, 0

Appendix E: Superlinear T -dependence

The difference between two γ -functions appearing in eq.(61) becomes exponentially smaller with increasing β . Although this is balanced by the presence of exponential term therein, the different series approximations of γ -functions mentioned below eq.(62) are no longer appropriate. Although technically complicated, a better approximation of C_v can be given as follows. Taking log of eq.(61) and using the approximation $\log(1+y) \approx y + \frac{y^2}{2} + \dots$,

$$\log\langle Z \rangle \approx \frac{\sqrt{\eta^3}}{\pi \sqrt{27} \lambda_0^3} \left(\frac{1}{x} \right)^{3/2} \left(\Gamma\left(\frac{3}{2}, x\right) - \Gamma\left(\frac{3}{2}, (1+\eta^{-1})x\right) \right) e^x \quad (E1)$$

with $\Gamma(a, x) = 1 - \gamma(a, x)$ and $x = \eta\beta e_0$. Further using the relation $\frac{\partial \Gamma(a, x)}{\partial x} = -x^{a-1} e^{-x}$, eq.(49) then gives

$$C_v(T) \approx \frac{k_b \sqrt{2\eta^3}}{\pi \sqrt{27} \lambda_0^3} \frac{1}{x^{3/2}} \left[(15/4 - 3x + x^2) \left(\Gamma\left(\frac{3}{2}, (1+\eta^{-1})x\right) - \Gamma\left(\frac{3}{2}, x\right) \right) e^x + \right. \\ \left. - \frac{(1+\eta)^{3/2}}{2\eta^{5/2}} (6\eta - \eta x + 4x^2) x^{1/2} e^{-x/\eta} + \frac{1}{2} x^{3/2} (1-x) \right] \quad (E2)$$

The power of the leading term of $C_v(T)$ can now be seen by calculating the local power law exponent $\alpha = \frac{d \log C_v}{d \log T}$. Following from eq.(E2), α varies between $1 \rightarrow 1.5$ as T varies.

TABLE III: Refractive indices of glasses [69]: here columns 2 – 7 give the refractive indices, of the glasses listed in 1st column, for the given wavelength (in μm), with $\lambda_1 = 0.6328$, $\lambda_2 = 0.5893$, $\lambda_3 = 0.5876$, $\lambda_4 = 0.5461$, $\lambda_5 = 0.4800$, $\lambda_6 = 0.4358$

Glass	λ_1	λ_2	λ_3	λ_4	λ_5	λ_6
a-SiO2			1.4585			1.4667
BK7	1.5151	1.5168		1.5187	1.5228	1.5267
As2S3	2.465	2.48	2.521	2.5620	2.636	
LASF7		1.850				
SF4		1.7551	1.7912			
SF59	1.9432	1.962	1.9635	1.9890	2.0156	
a-Se			2.4153			2.45
Se75Ge25			2.9733			2.6554
Se60Ge40			3.2734			2.79
LiCl:7H2O			1.3939			1.4013
Zn-Glass			1.5281			
ET1000			1.4585			1.4667
:						

TABLE IV: Refractive indices of Polymers [69]: here each column gives the refractive indices of the listed polymers for the given wavelength (in μm), with $\lambda_1 = 1.0520$, $\lambda_2 = 0.8790$, $\lambda_3 = 0.8330$, $\lambda_4 = 0.7030$, $\lambda_5 = 0.6328$, $\lambda_6 = 0.5893$, $\lambda_7 = 0.5876$, $\lambda_8 = 0.4861$, $\lambda_9 = 0.4368$

Glass	λ_1	λ_2	λ_3	λ_4	λ_5	λ_6	λ_7	λ_8	λ_9
PMMA	1.481	1.483	1.484	1.486	1.489	1.491	1.491	1.497	1.502
PS	1.576	1.576	1.577	1.575	1.587	1.589	1.592	1.606	1.617
PC	1568	1.568	1.569	1.582	1.580	1.586	1.585	1.599	1.612

Appendix F: Contribution of higher order plets in eq.(11)

To gain a better insight, it is instructive to write eq.(11) explicitly for first few p -plets i.e $p = 0, 1, 2$,

$$\mathcal{U}_{KL} \approx \mathcal{U}_{KK}^{es} \quad 0 - plet, \mathcal{K}_r = \mathcal{L}_r \forall r = 1 \rightarrow g_0 \quad (F1)$$

$$\approx \sum_{n=1}^{g_0} \mathcal{U}_{KL}^{(mn)} + \sum_{n,r=1}^{g_0} \mathcal{U}_{KL}^{(mnr)} + .. \quad 1 - plet, \mathcal{K}_m \neq \mathcal{L}_m, \quad (F2)$$

$$\approx \mathcal{U}_{KL}^{(mn)} + \sum_{r=1}^{g_0} \mathcal{U}_{KL}^{(mnr)} + \sum_{r,s=1}^{g_0} \mathcal{U}_{KL}^{(mnrs)} + .. \quad 2 - plet, \mathcal{K}_{m,n} \neq \mathcal{L}_{m,n} \quad (F3)$$

As clear from the above, \mathcal{U}_{KL} connecting a basis-pair \mathcal{K}, L forming a p -plet (for $p > 0$) has contribution from all $p+x$ body terms with $x \geq 0$ (i.e $p \leq p+x \leq g_0$). As a consequence of the above, the significant contribution to v_{kl} in eq.(14) comes only from the square of many body terms; it can be written as

$$v_{KL} \approx \sum_{n=1}^{g_0} \langle E_{\mathcal{K}_n}^2 \rangle + \langle (\mathcal{U}_{\mathcal{K}_K})^2 \rangle \quad 0 - plet, \mathcal{K}_r = \mathcal{L}_r \forall r = 1 \rightarrow g_0 \quad (F4)$$

$$\approx \sum_{n=1}^{g_0} \langle (\mathcal{U}_{KL}^{(mn)})^2 \rangle + \sum_{n,r=1}^{g_0} \langle (\mathcal{U}_{KL}^{(mnr)})^2 \rangle + .. \quad 1 - plet, \mathcal{K}_m \neq \mathcal{L}_m, \quad (F5)$$

$$\approx \langle (\mathcal{U}_{KL}^{(q1,...,qp)})^2 \rangle + \sum_{r=1}^{g_0} \langle (\mathcal{U}_{KL}^{(q1,...,qp,r)})^2 \rangle + \sum_{r,s=1}^{g_0} \langle (\mathcal{U}_{KL}^{(q1,...,qp,r,s)})^2 \rangle + ..$$

$$p - plet, \mathcal{K}_{q1,q2,...,qp} \neq \mathcal{L}_{q1,q2,...,qp} \quad (F6)$$

As clear from the above, v_{kl} for a p -plet consists of the many body contributions among p or more molecules. Thus variances of the matrix elements corresponding to higher-plets are relatively weaker as compared to lower ones. But as number of p -plets increases with p , their collective contribution need not be negligible.

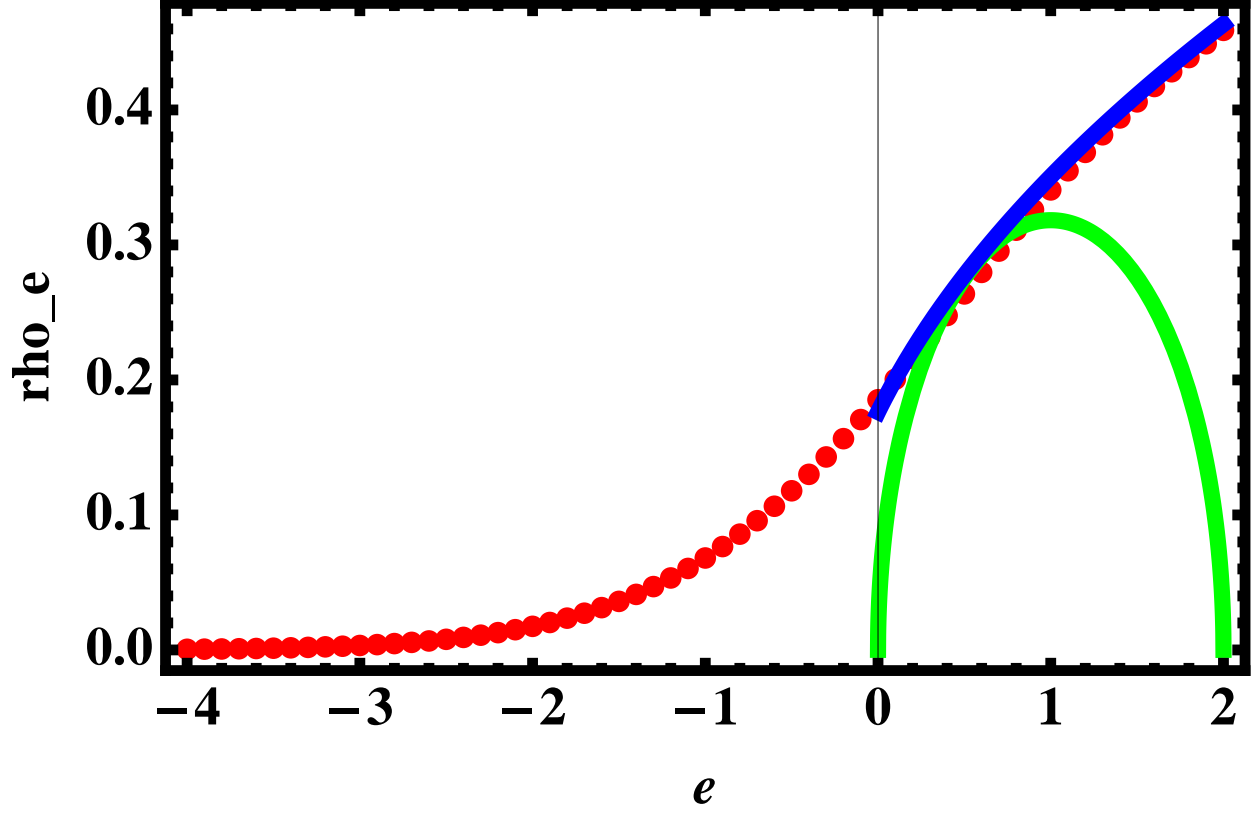


FIG. 1: **Finding e_0 where edge meets bulk?:** Bulk density of state $\rho_{bulk}(e)$ (eq.(38), green color) and the edge density of states $\rho_{edge}(e)$ (eq.(39) with $f(x)$ given by eq.(40), red dots). The approximation (44) of $\rho_{edge}(e)$ for $e > 0$ is also depicted by blue color.

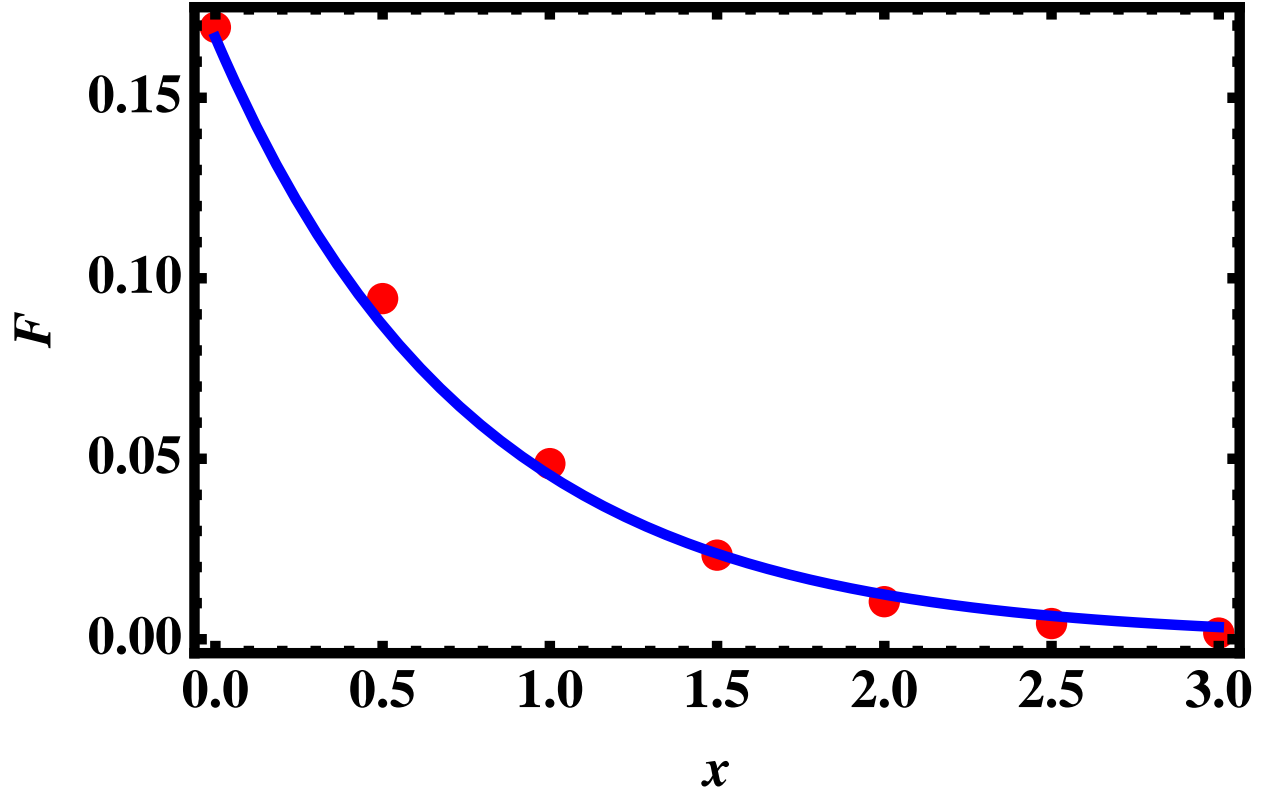


FIG. 2: **Counting function** $\mathcal{F}(x) = \int_{-\infty}^x dx f_L(x)$ (see eq.(47)): A rapid exponential decay of $\mathcal{F}(\lambda b_0 e)$ (red dots) away from $e = 0$ indicates most of the eigenvalues lie close to $e = 0$. The solid curve (blue color) describes the fit $(1/6)\exp[-1.3 x]$.

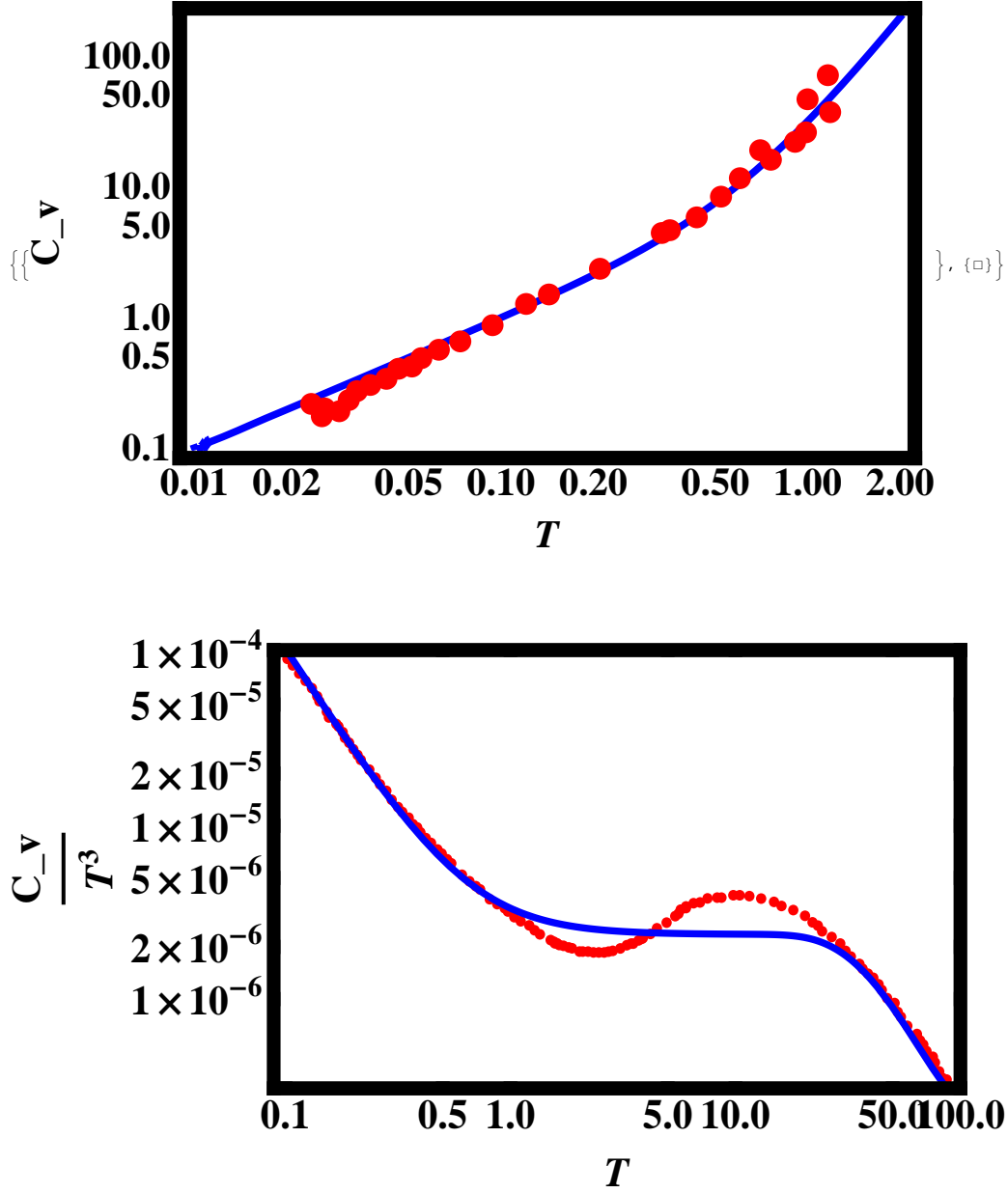


FIG. 3: Comparison of total specific heat of a basic block with experimental data: $c_v^{total} = c_v + c_v^{ph}$, with $c_v = \frac{1}{\rho_m \Omega_b} \langle C_v \rangle$ obtained from eqs.(60, 49) and c_v^{ph} from eq.(73) is displayed by the blue curve. Experimental data for Suprasil (red curve) is taken from figure 6 of [38] for *Top* case and from figure 1 of [38] for *bottom* case. The T_D value which seems to give a better fit in this case is much less than that of bulk; here $T_D = 190^\circ\text{K}$. Note $T_D \approx 495^\circ\text{K}$ for the macroscopic sizes of $a - \text{SiO}_2$ [2].

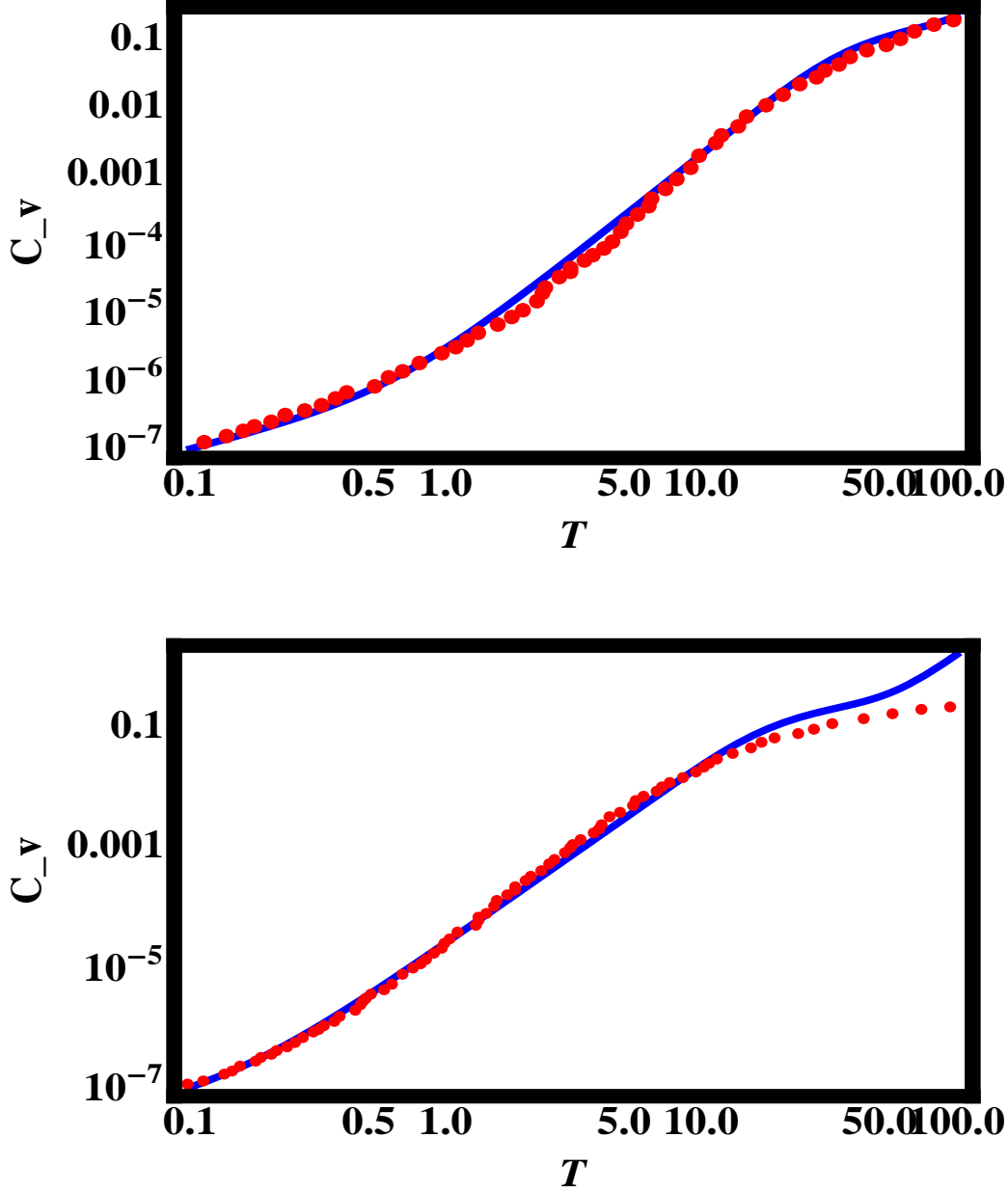


FIG. 4: Comparison of total specific heat with experimental data: $c_v^{total} = c_v + c_v^{ph}$, with c_v obtained from eqs.(60, 49) and c_v^{ph} from eq.(73), is displayed by the blue curve. *Top*: $a - SiO_2$ with $T_D = 200^\circ\text{K}$, *Bottom*: vitreous Se with $T_D = 113^\circ\text{K}$. Experimental data (red curve) for $a - SiO_2$ and vitreous Se is taken from figure and figure 12 of [1], respectively. The T_D value which seems to give a better fit in both cases is less than that of bulk. Note $T_D \approx 200^\circ\text{K}$ and 123°K for the macroscopic sizes of $a - SiO_2$ and $a - Se$ [2].